9TH INTERNATIONAL WORKSHOP ON RELIABLE ENGINEERING COMPUTING
Risk and Uncertainty in Engineering Computations
Virtual Conference: May 17-20, 2021
REC 2021

UNIVERSITY OF MESSINA

UNIVERSITY "MEDITERRANEA" OF REGGIO CALABRIA

Using a Tuned Fluid Inerter for Improving the Seismic Performance of Structures Isolated with Friction Pendulum System

Dario De Domenico, Giuseppe Ricciardi

Department of Engineering,
University of Messina, Italy
dario.dedomenico@unime.it

Università degli Studi di Messina
DIPARTIMENTO DI INGEGNERIA

Traditional Base Isolation System (BIS)

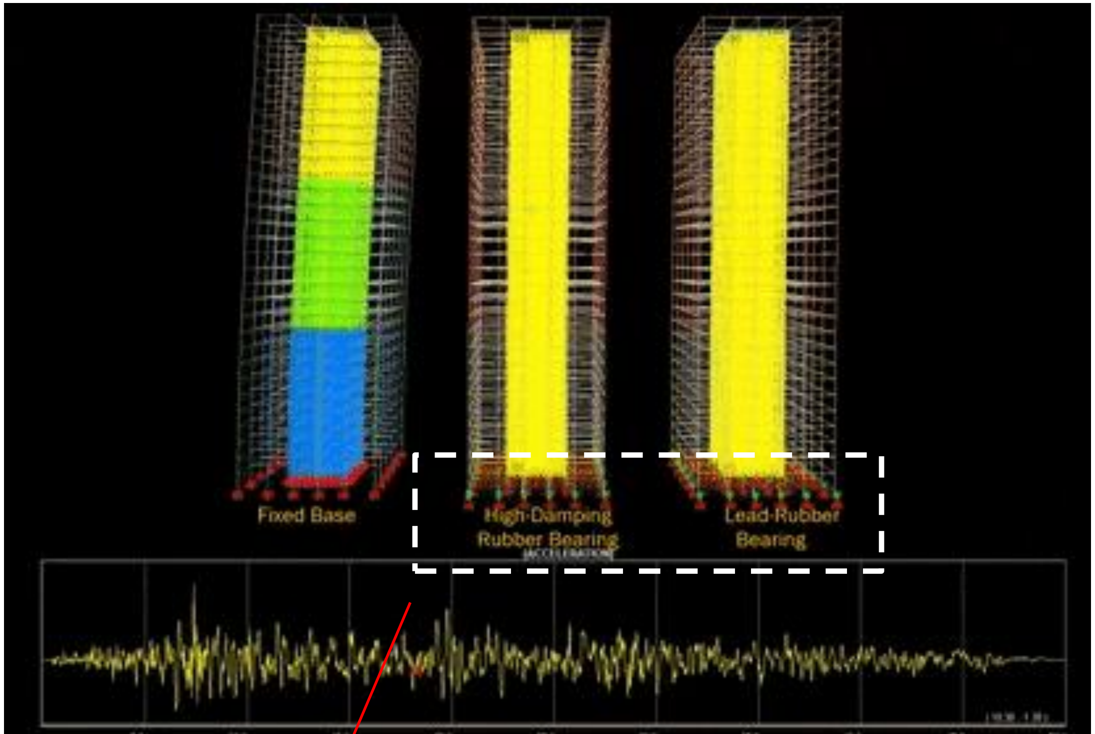

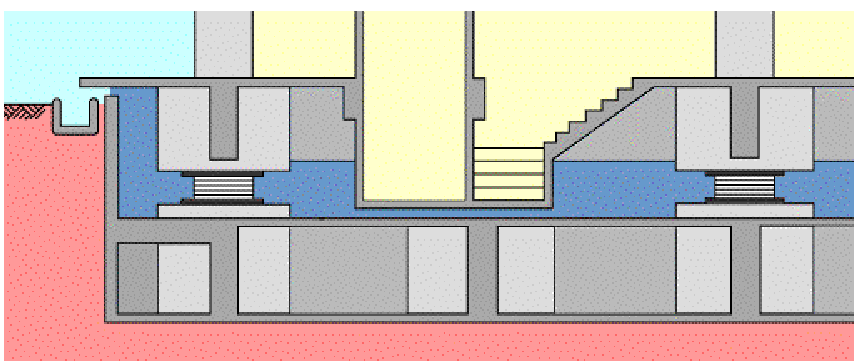

Rubber bearings (HDRB and LDRB)

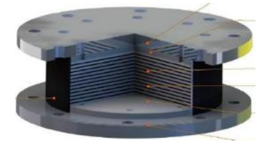

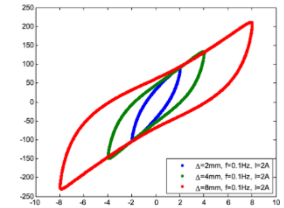

LRB isolator

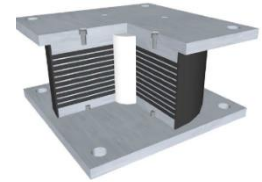

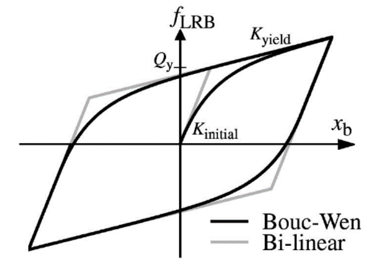

FPS isolator

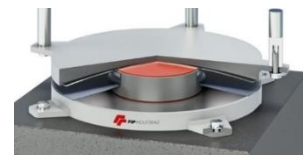

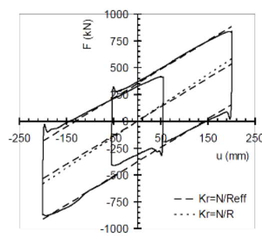

TFP - Triple

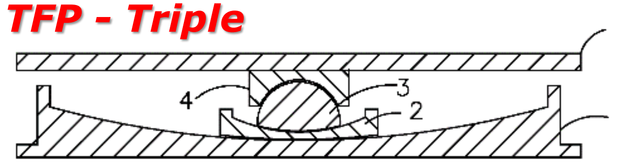

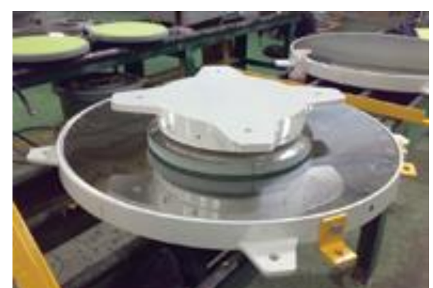

Flat slides

What is the need for innovative isolation systems??

1) Large displacements imply large isolators…

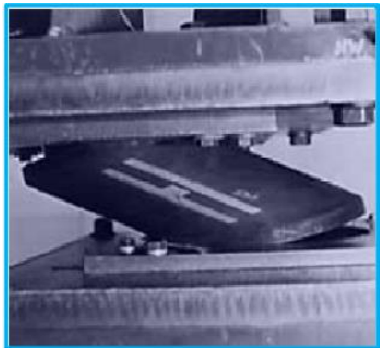

2) Costly flexible connections for utilities…

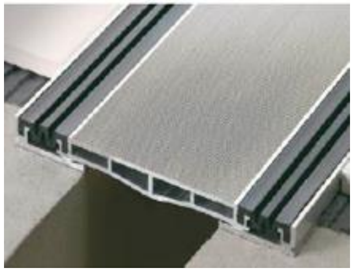

3) Risk of mutual collisions and pounding for adjacent buildings…

The 1985 Mexico Earthquake (Anagnostopoulos 1988)

The 1985 Mexico earthquake (Johnmartin 2018, NCEI 2018)

The 2011 Van earthquake (Ozmen et al. 2013, Aykutozdemir 2018)

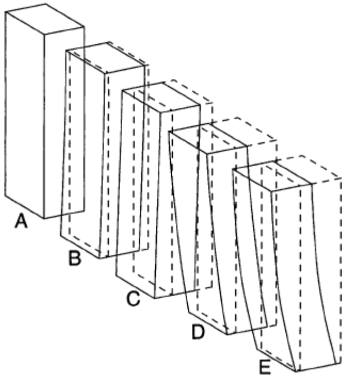

What is the need for innovative isolation systems??

*4) Vulnerability to **near-fault and long-period ground motions**, which trigger resonance phenomena and amplify the displacements beyond the design value*

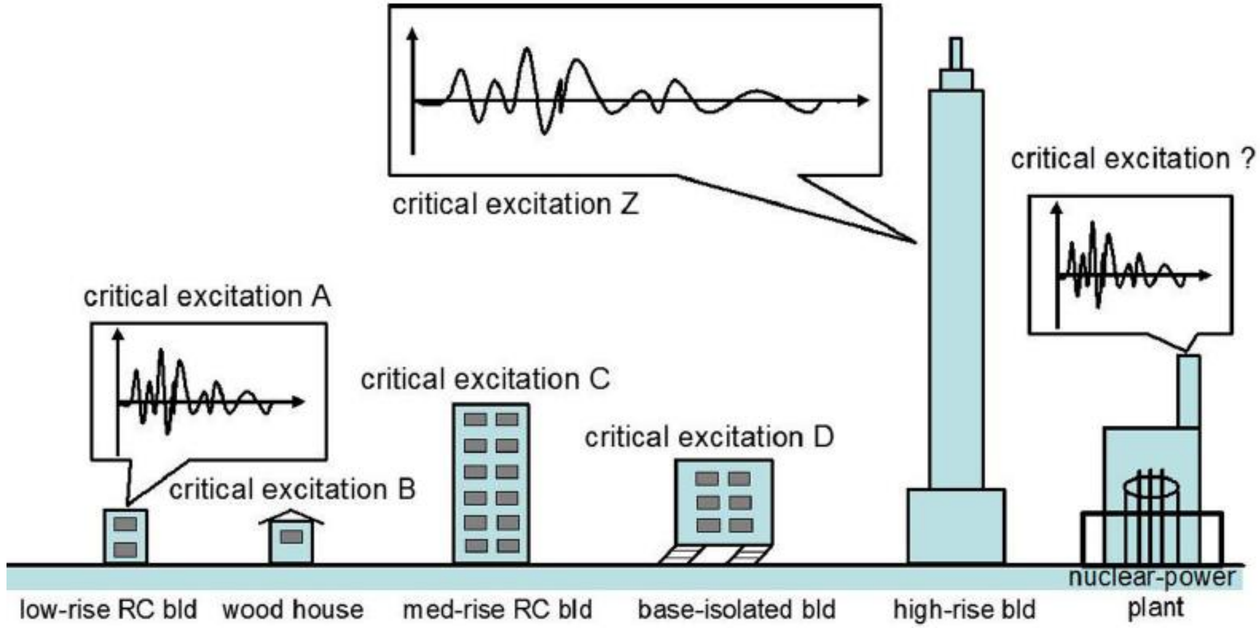

Heaton TH, Hall JF,Wald DJ, Halling MW. Response of high-rise and base-isolated buildings to a hypothetical Mw 7.0 blind thrust earthquake. Science 1995; 267:206–211.
Ariga T, Kanno Y, Takewaki I. Resonant behaviour of base-isolated high-rise buildings under long-period ground motions. Struct Des Tall Spec Build 2006; 15:325–338.
Takewaki I, Murakami S, Fujita K, Yoshitomi S, Tsuji M. The 2011 off the Pacific coast of Tohoku earthquake and response of high-rise buildings under long-period ground motions. Soil Dyn Earth Eng 2011; 31:1511–1528

Combined Isolation Technologies: BIS + dampers

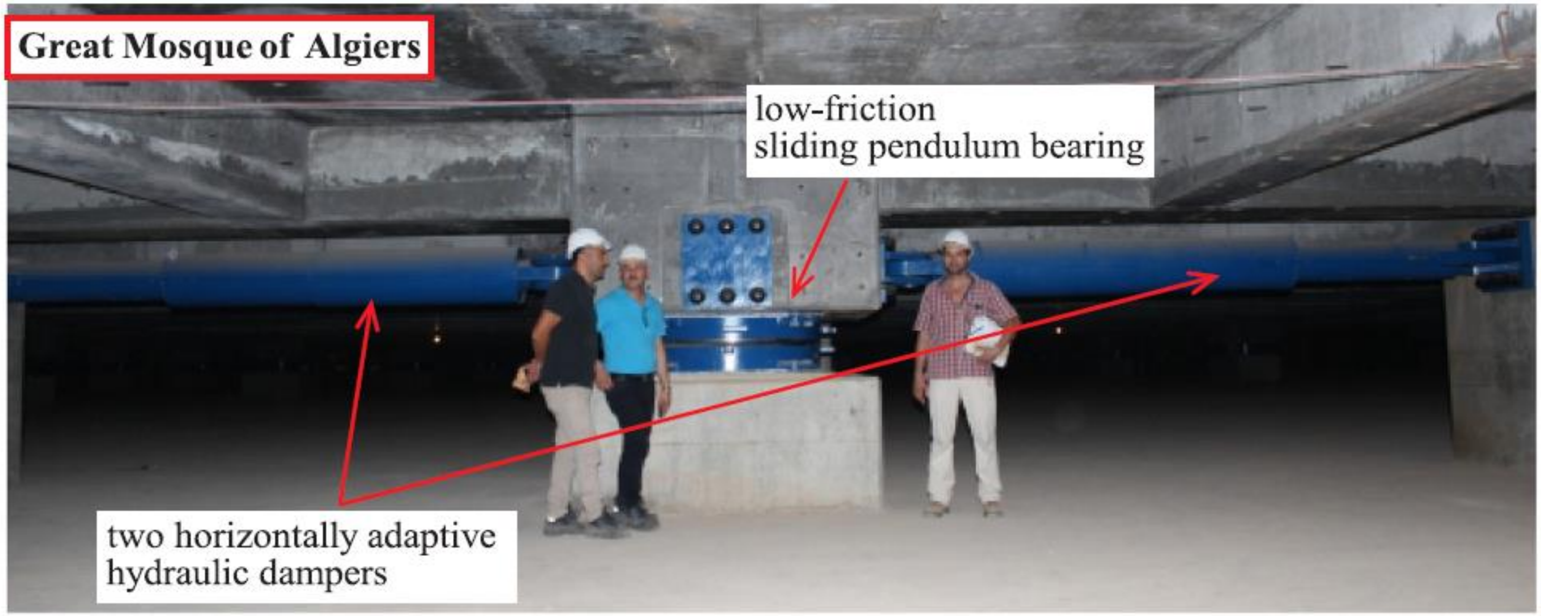

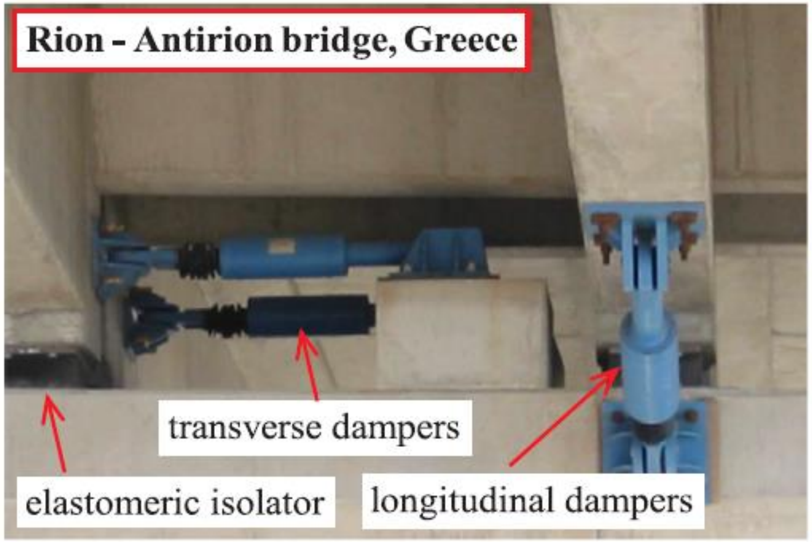

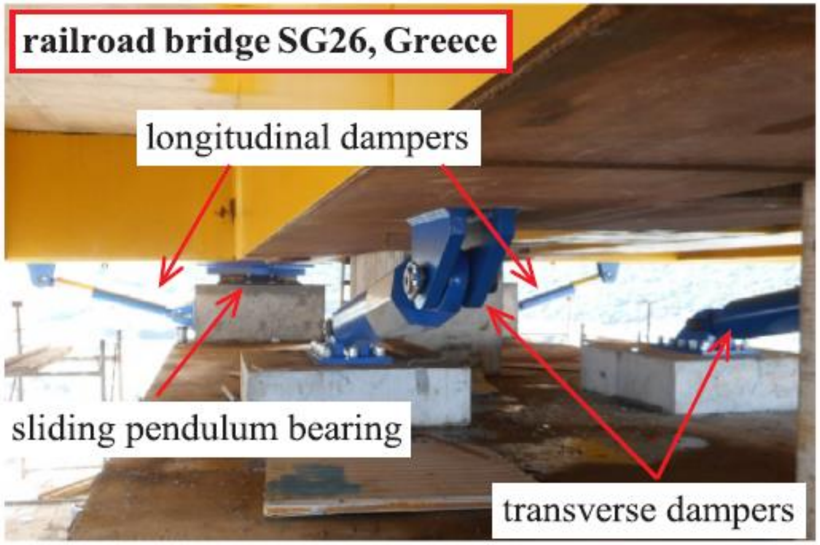

Combined Isolation Technologies: BIS + SMA gap dampers

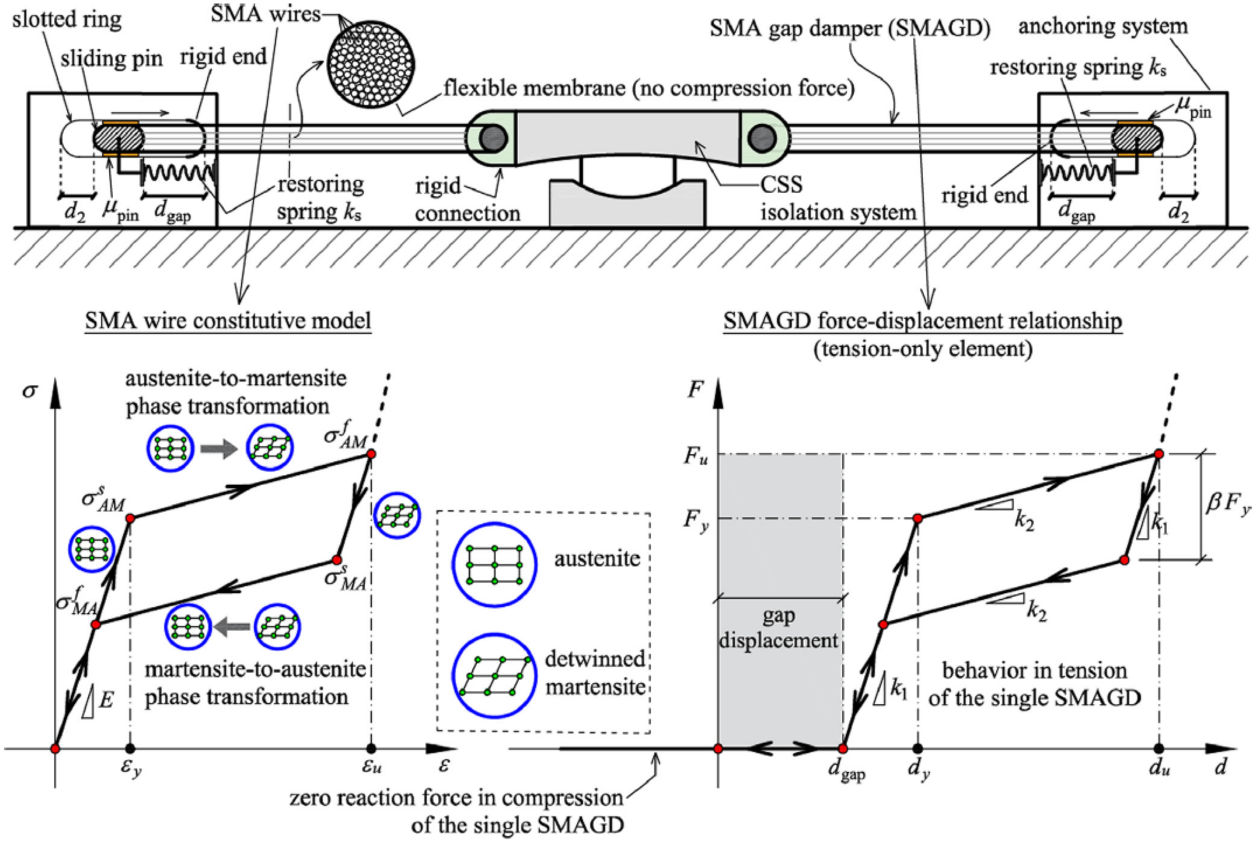

Low-friction curved surface slider (CSS) combined with shape memory alloy (SMA) gap dampers

De Domenico, Gandelli & Quaglini (2020) Eng Struct 212; 110536

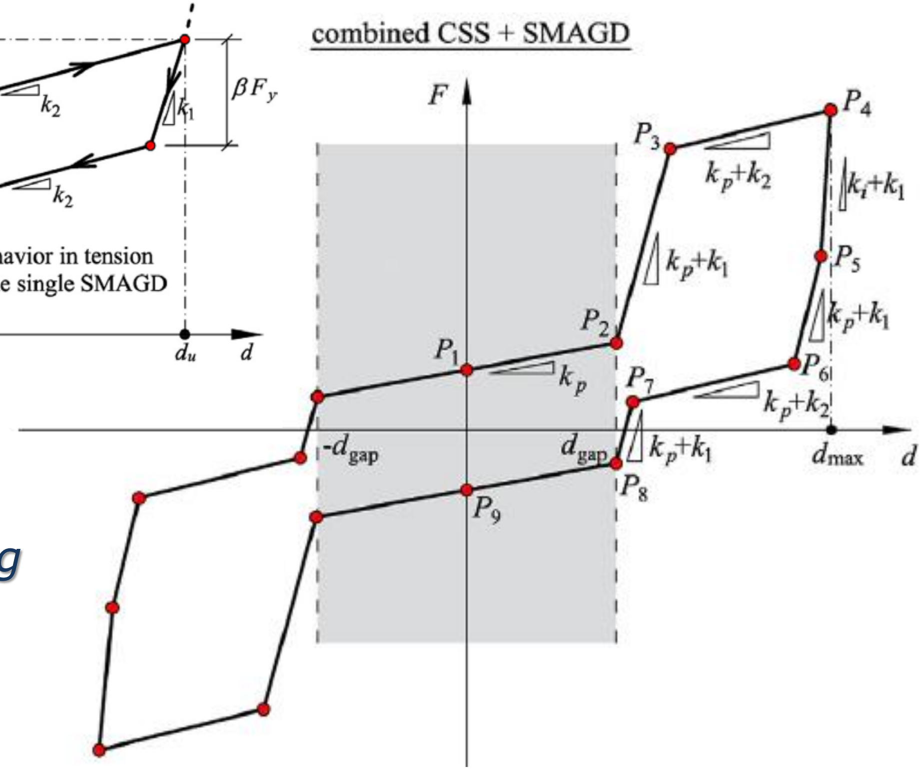

Flag-shaped hysteresis of SMAs provides additional energy dissipation and stiffening without implying residual displacements

Combined Isolation Technologies: BIS + SMA gap dampers

Low-friction curved surface slider (CSS) combined with shape memory alloy (SMA) gap dampers

De Domenico, Gandelli & Quaglini (2020) Eng Struct 212; 110536

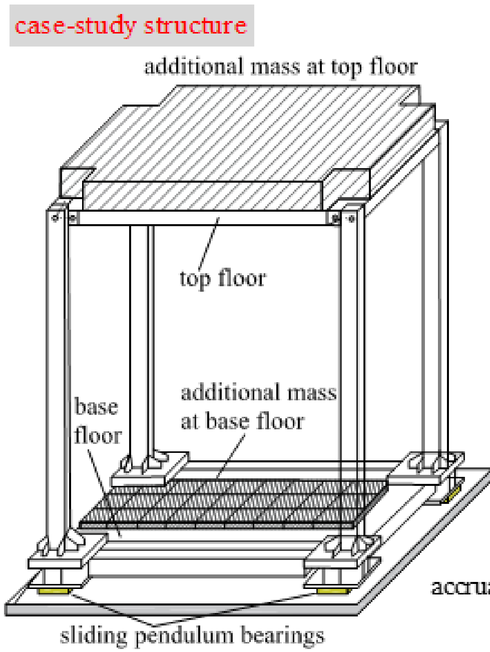

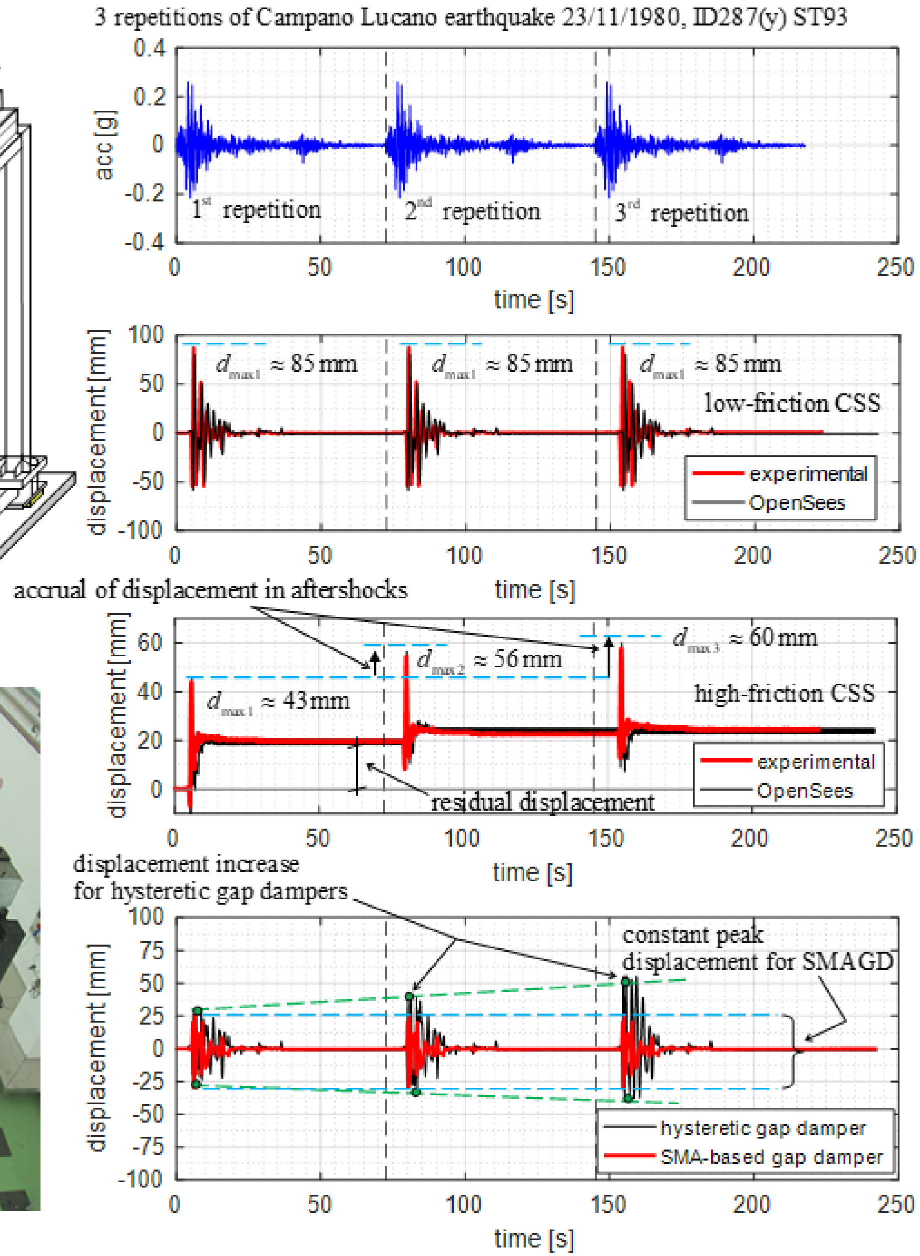

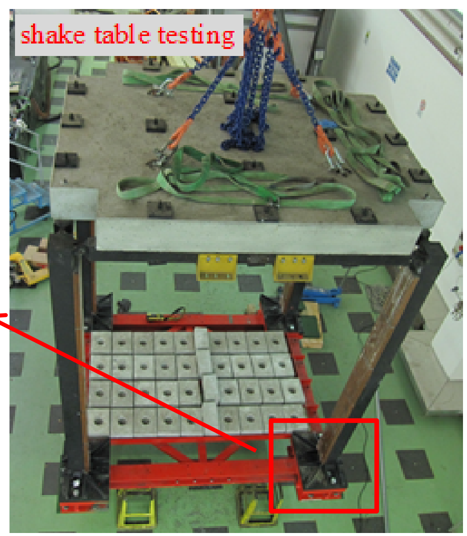

Combined Isolation Technologies: BIS + SMA gap dampers

Low-fri curved slider (combin shape alloy (S dampe

De Dome Gandelli & Quaglini (Eng Struc 110536

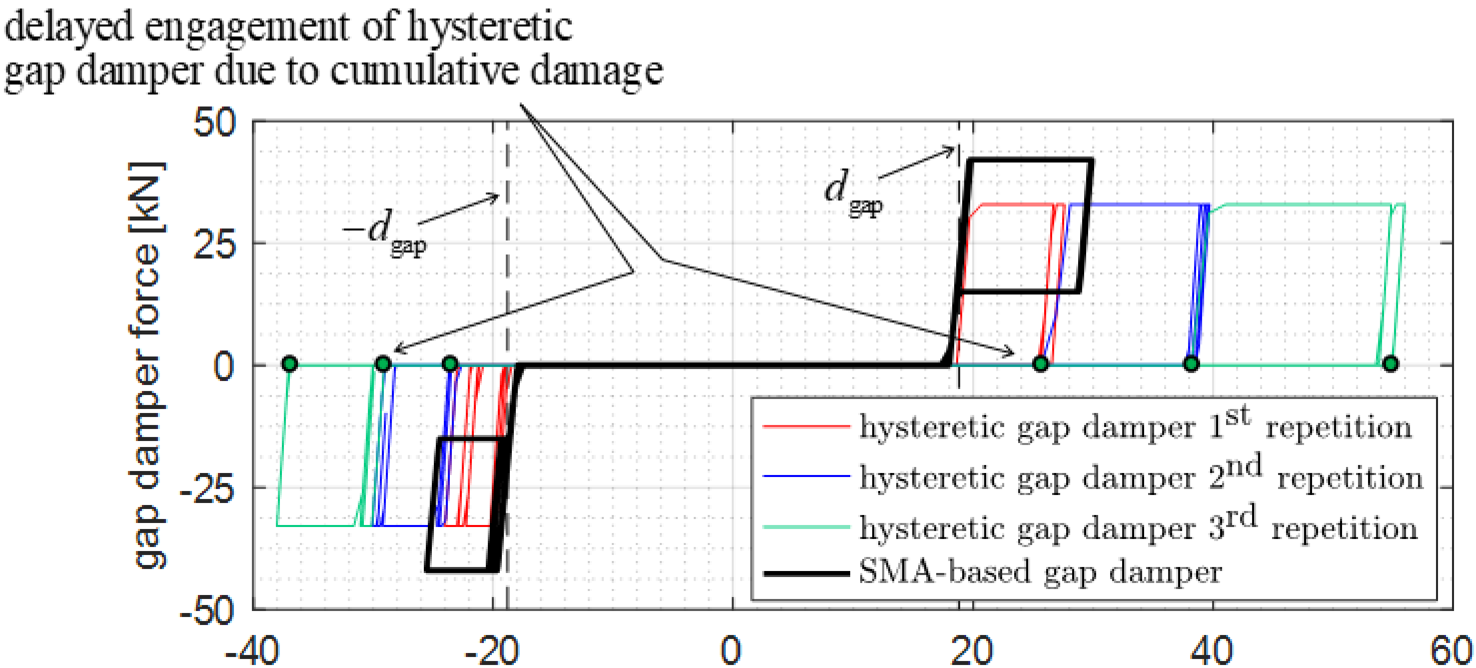

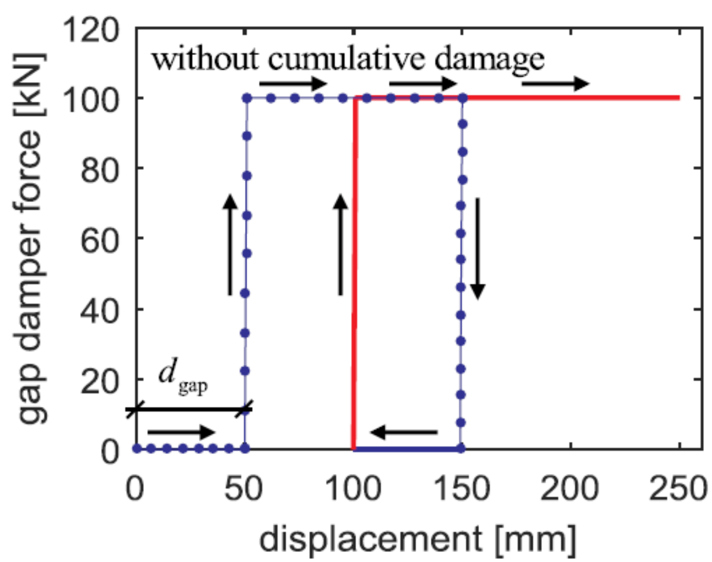

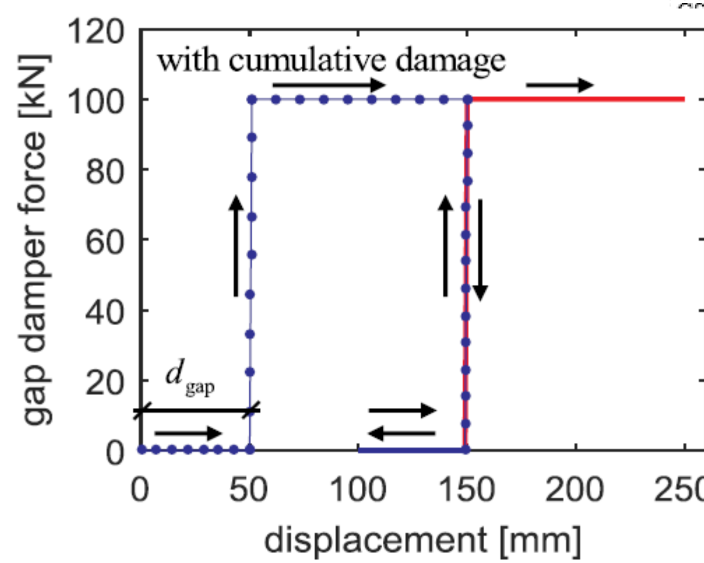

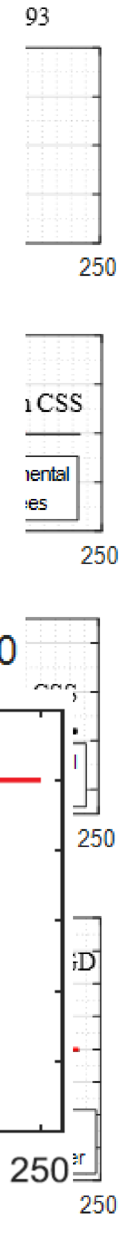

Combined Isolation Technologies: BIS + SMA gap dampers

Low-friction curved surface slider (CSS) combined with shape memory alloy (SMA) gap dampers

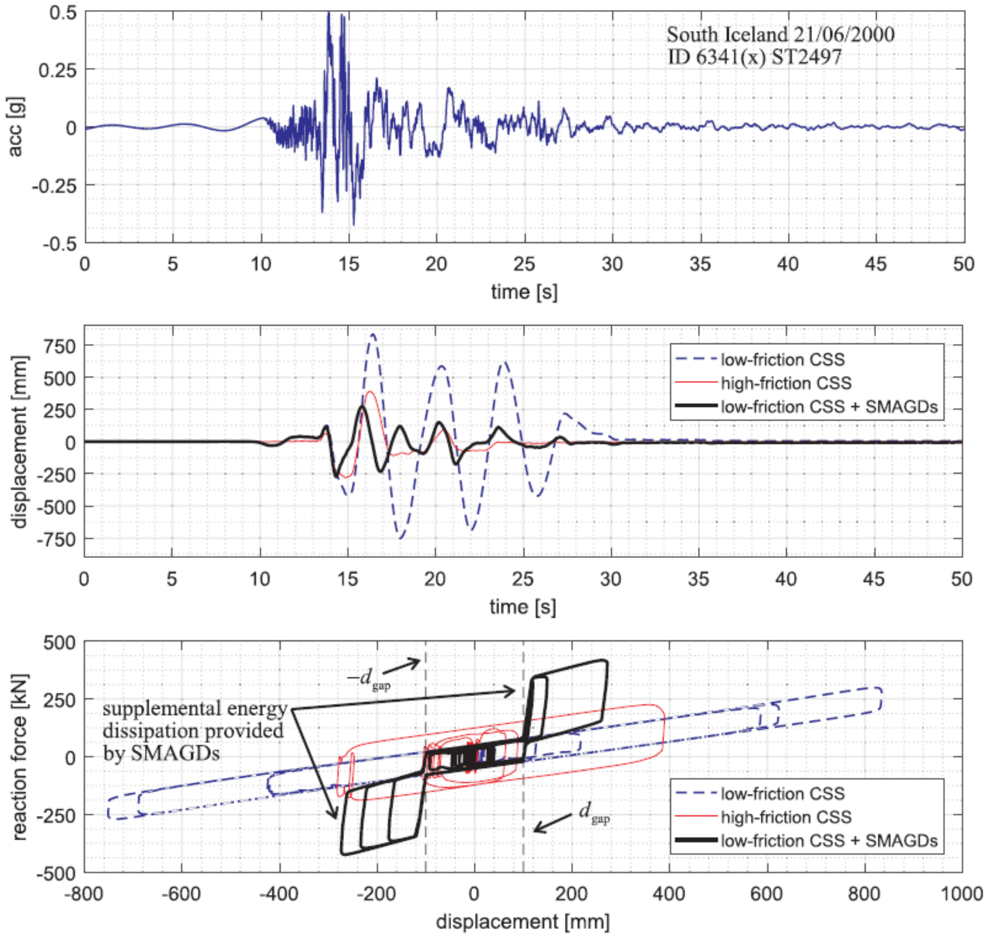

Maximum credible earthquake

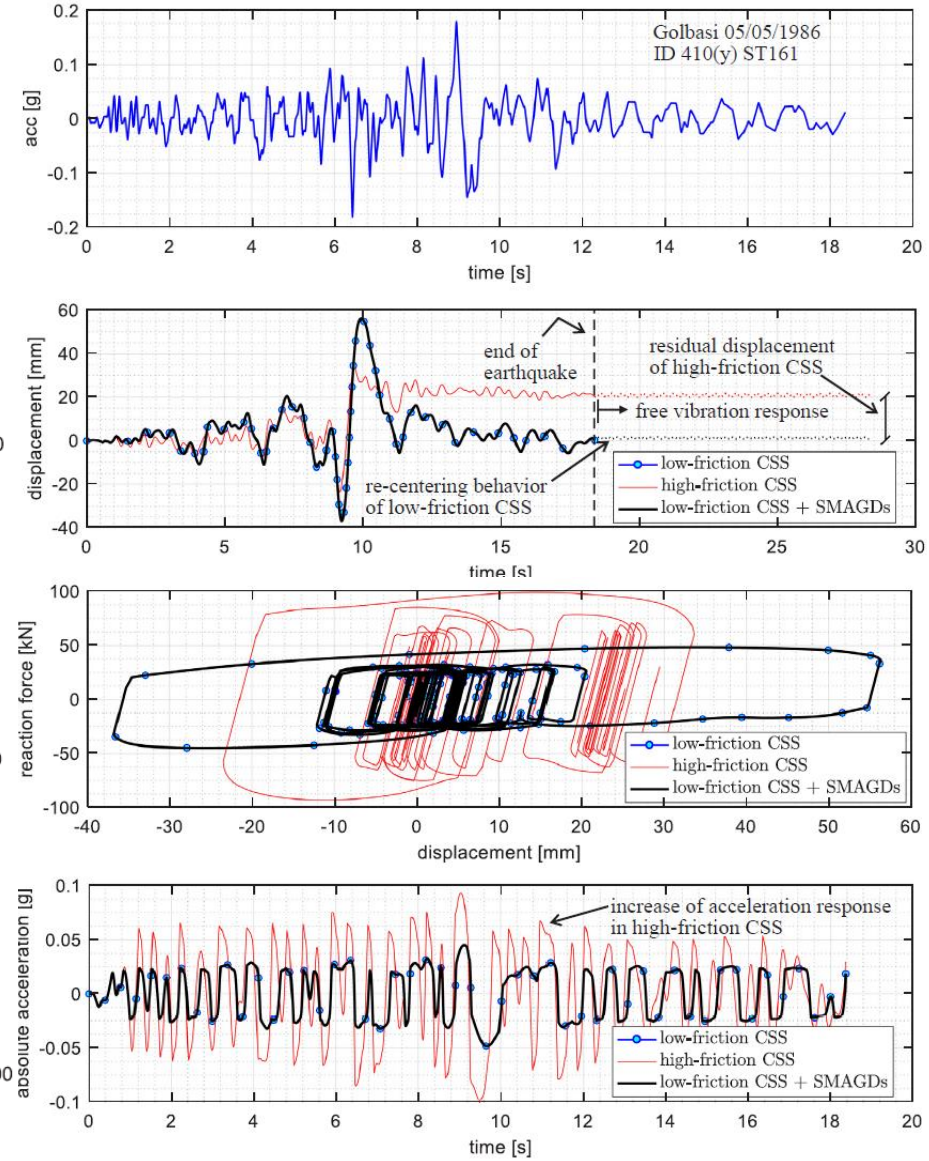

Serviceability (frequent) earthquake

Tuned Mass Damper (TMD)

Taipei 101's tower: H=500 m; Mass TMD= 730ton
Resisted a 6.8 Richter earthquake

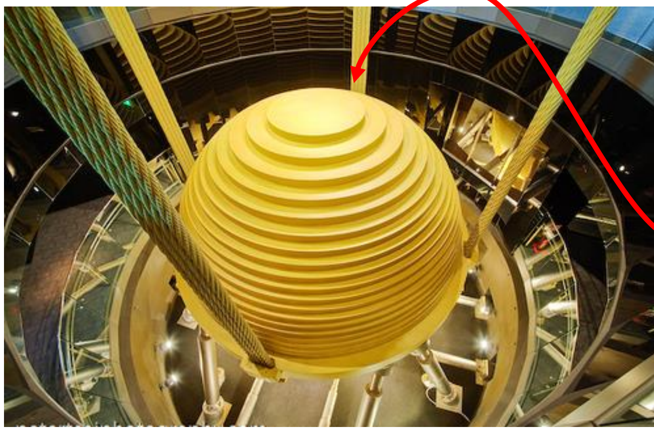

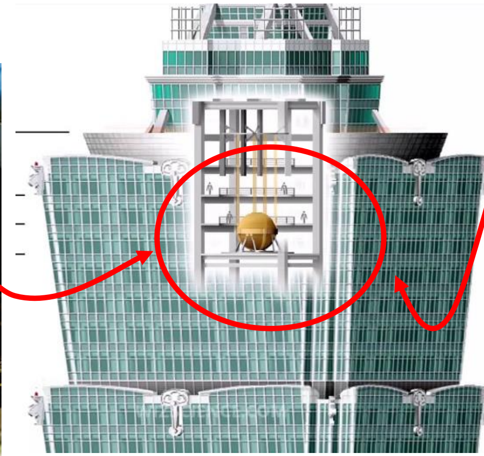

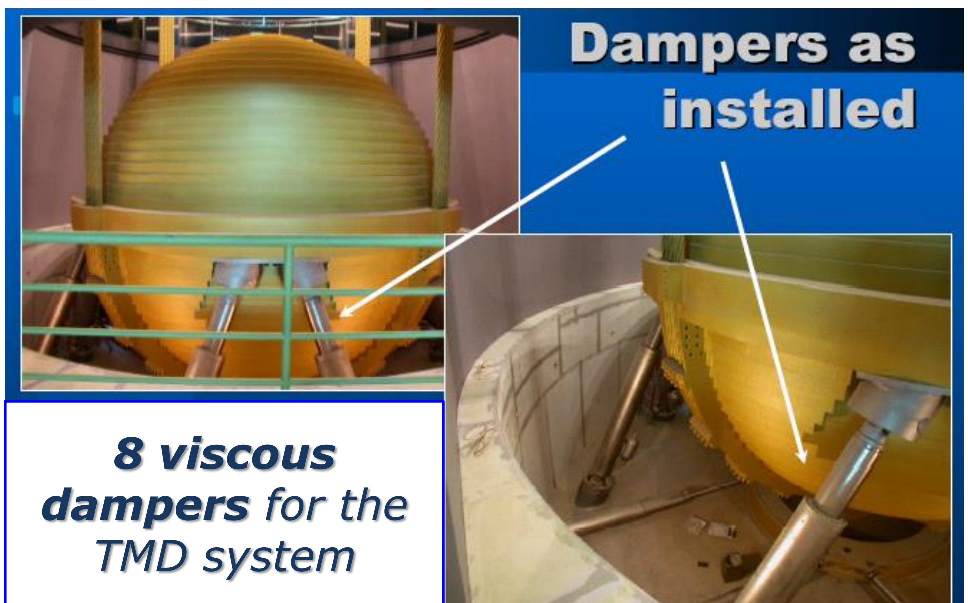

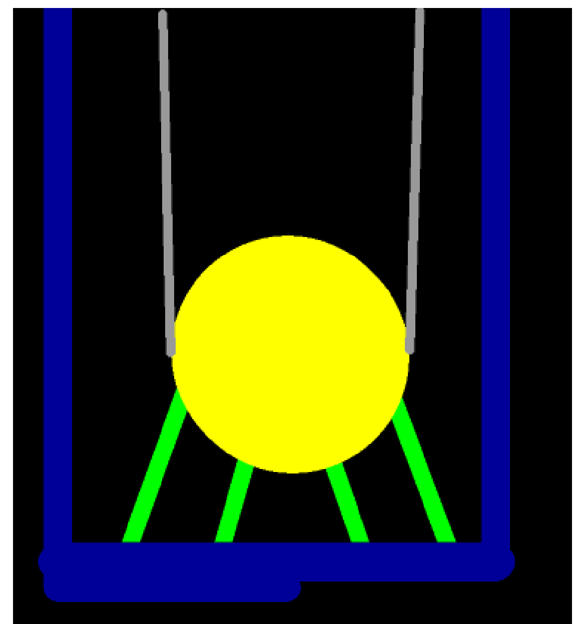

Combined Isolation Technologies: BIS + TMD

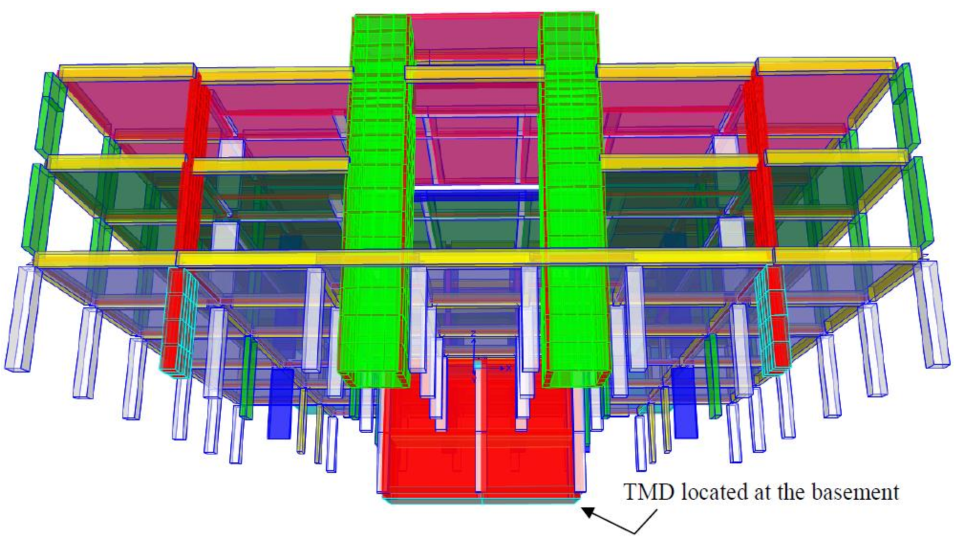

Low-damping rubber bearings combined with Tuned Mass Damper (TMD) at basement

De Domenico & Ricciardi (2018)
Soil Dyn Earth Eng 113; 503-521

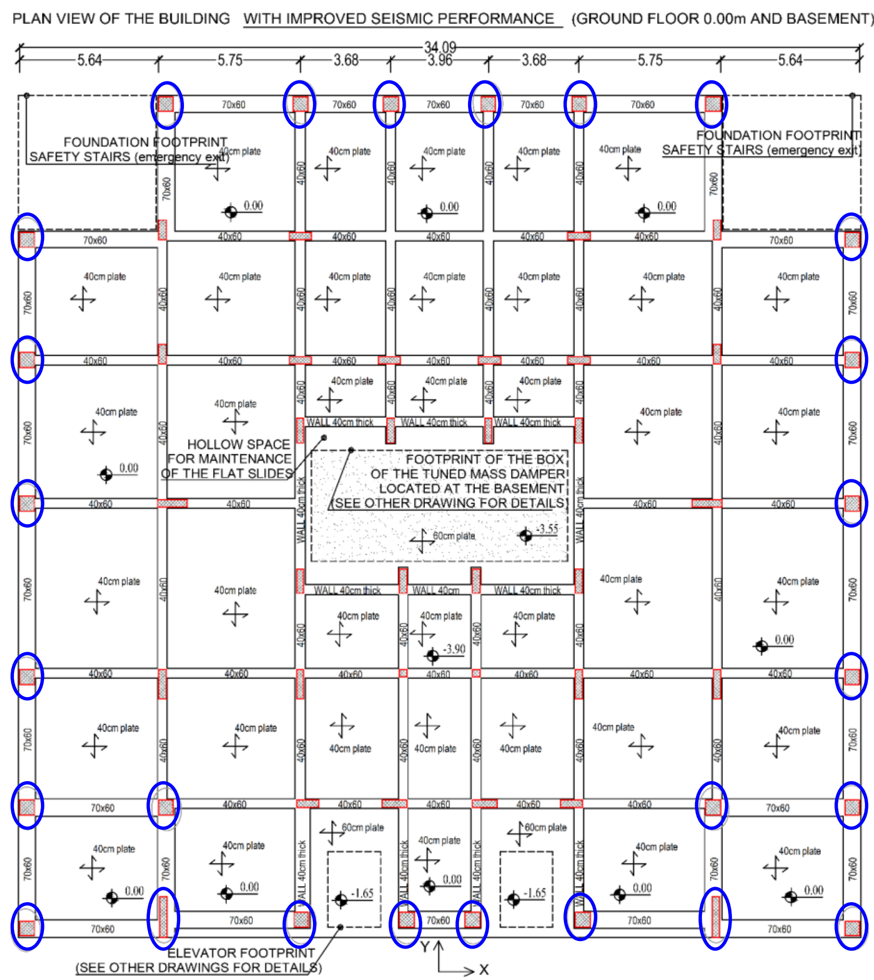

Combined Isolation Technologies: BIS + TMD

The structure is base isolated and an additional TMD is located at the basement of the building (to reduce the displacement demand and improve the seismic performance)

Low-damping rubber bearings combined with Tuned Mass Damper (TMD) at basement

De Domenico & Ricciardi (2018)
Soil Dyn Earth Eng 113; 503-521

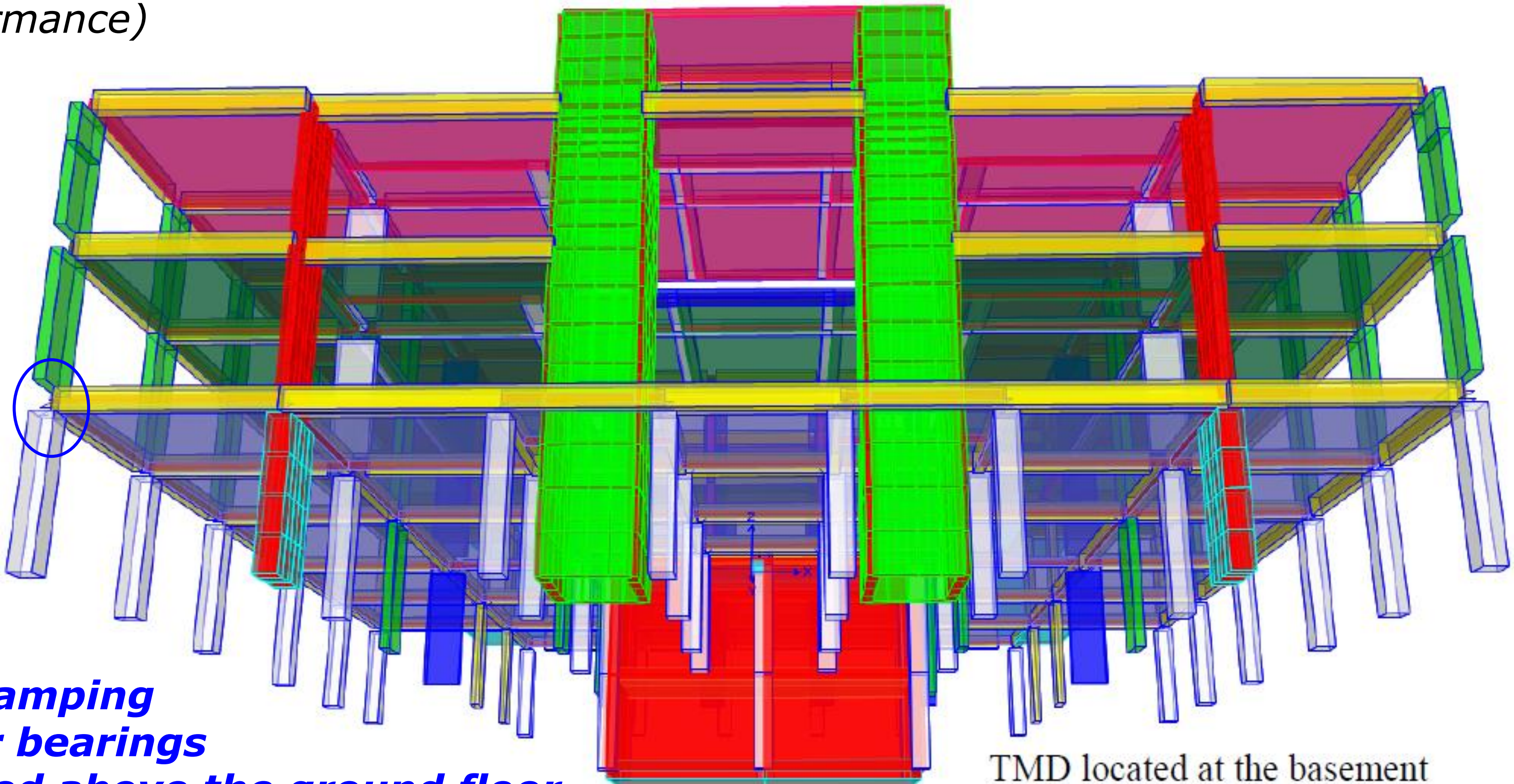

Low-damping rubber bearings installed above the ground floor

TMD located at the basement

Combined Isolation Technologies: BIS + TMD

Simplified 3DOF model

$$m_s\left(\ddot{u}_{sr}+\ddot{u}_b\right)+c_s\dot{u}_{sr}+k_s u_{sr}=-m_s\ddot{u}_g(t)$$

$$M_{tot}\ddot{u}_b+m_s\ddot{u}_{sr}+c_b\dot{u}_b+\hat{k}_b u_b-c_t\left(\dot{u}_t-\dot{u}_b\right)-\hat{k}_t\left(u_t-u_b\right)=-M_{tot}\ddot{u}_g(t)$$

$$m_t\ddot{u}_t+c_t\left(\dot{u}_t-\dot{u}_b\right)+\hat{k}_t\left(u_t-u_b\right)=-m_t\ddot{u}_g(t)$$

The dynamic parameters are evaluated by ad-hoc developed FE models!!

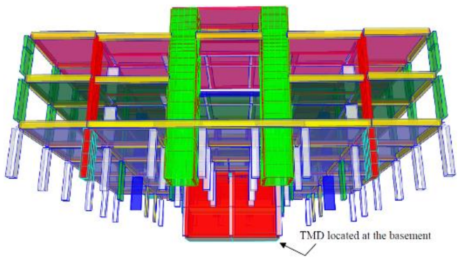

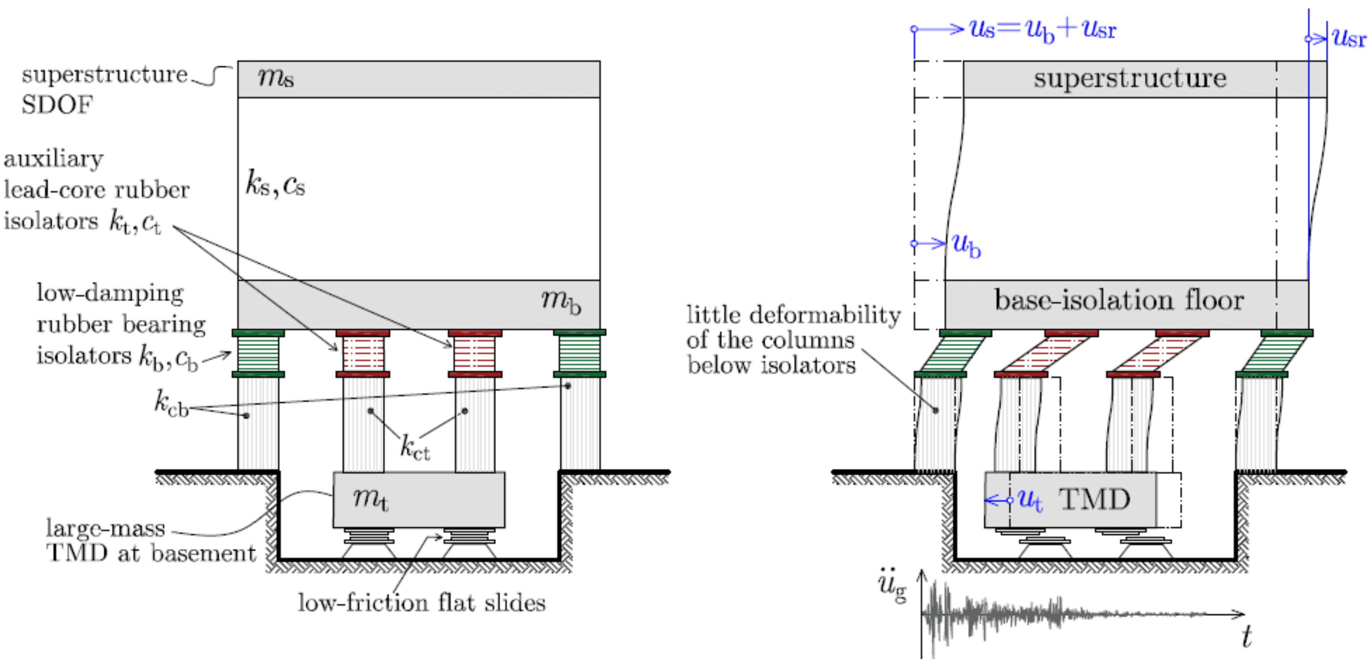

Mathematical model?

$$\hat{k}_b=\frac{k_{cb}k_b}{k_{cb}+k_b};\quad \hat{k}_t=\frac{k_{ct}k_t}{k_{ct}+k_t}$$

Deformability of the first-floor columns is incorporated in the simplified 3DOF model

in the limit case as $k_{cb}\rightarrow\infty$ and $k_{ct}\rightarrow\infty$ one has $\hat{k}_b\equiv k_b$ and $\hat{k}_t\equiv k_t$

Combined Isolation Technologies: BIS + TMD

Modal analysis of the base-isolated structure + TMD

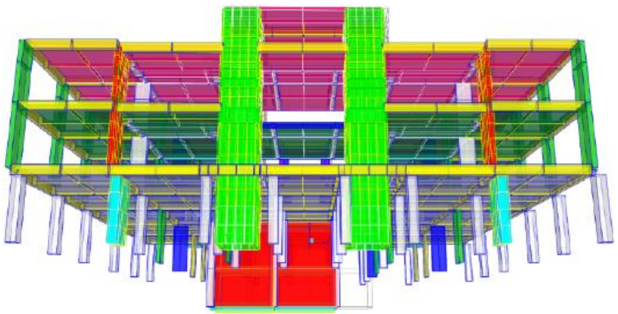

translational mode of the TMD (along X)
BIS is almost at rest

$T_1 = 4.54\,\mathrm{s}, \tilde{M}_{\%x} = 44\%, \tilde{M}_{\%y} = 0\%, \tilde{M}_{\%\theta} = 30\%$

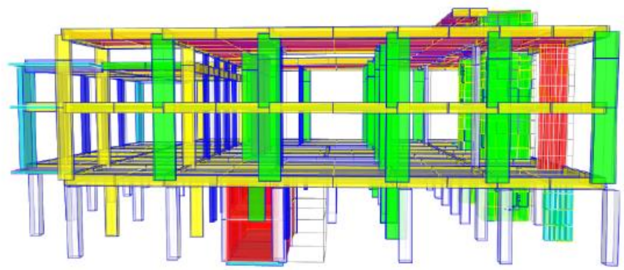

translational mode of the TMD (along Y)
BIS is almost at rest

$T_2 = 4.54\,\mathrm{s}, \tilde{M}_{\%x} = 0\%, \tilde{M}_{\%y} = 44\%, \tilde{M}_{\%\theta} = 0\%$

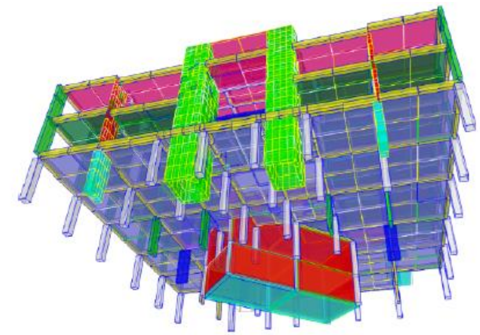

torsional mode of the TMD (rotation about Z)
BIS is almost at rest

$T_3 = 3.94\,\mathrm{s}, \tilde{M}_{\%x} = 0\%, \tilde{M}_{\%y} = 0\%, \tilde{M}_{\%\theta} = 1\%$

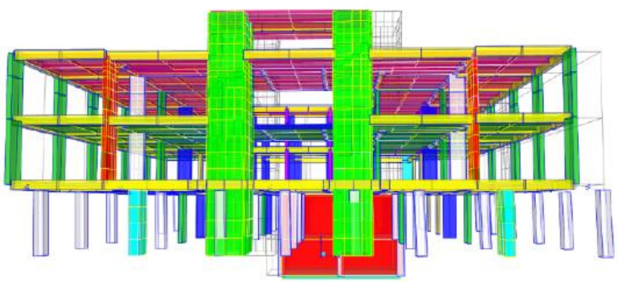

BIS
TMD

translational mode of the BIS (along X)
with TMD out of phase

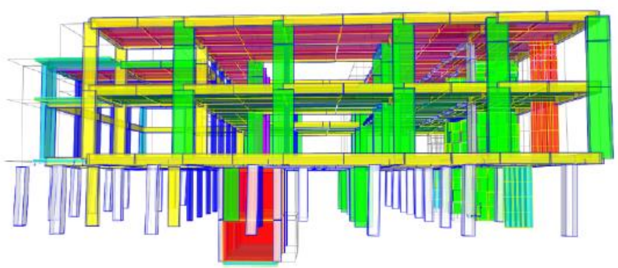

BIS
TMD

translational mode of the BIS (along Y)
with TMD out of phase

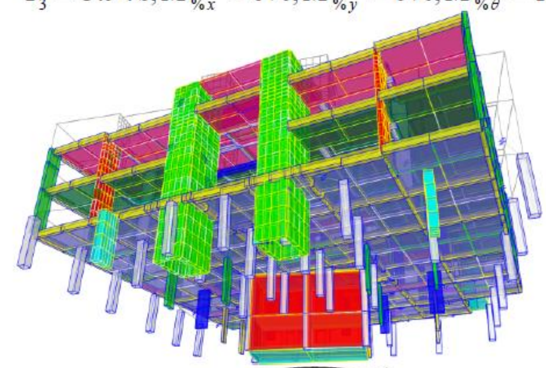

BIS
TMD

torsional mode of the BIS (rotation about Z)
with TMD out of phase

Combined Isolation Technologies: BIS + TMD

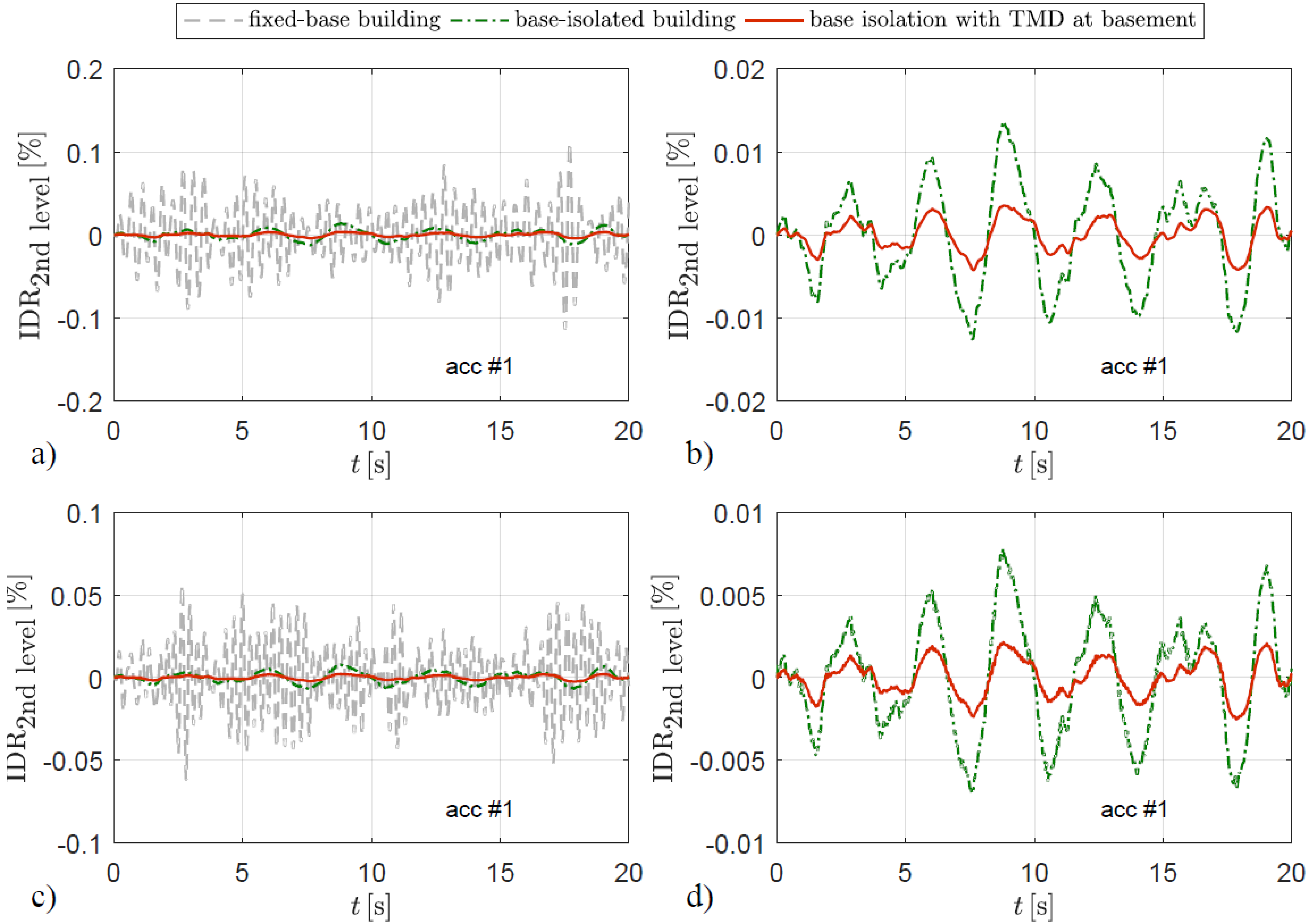

Combined Isolation Technologies: BIS + TMD

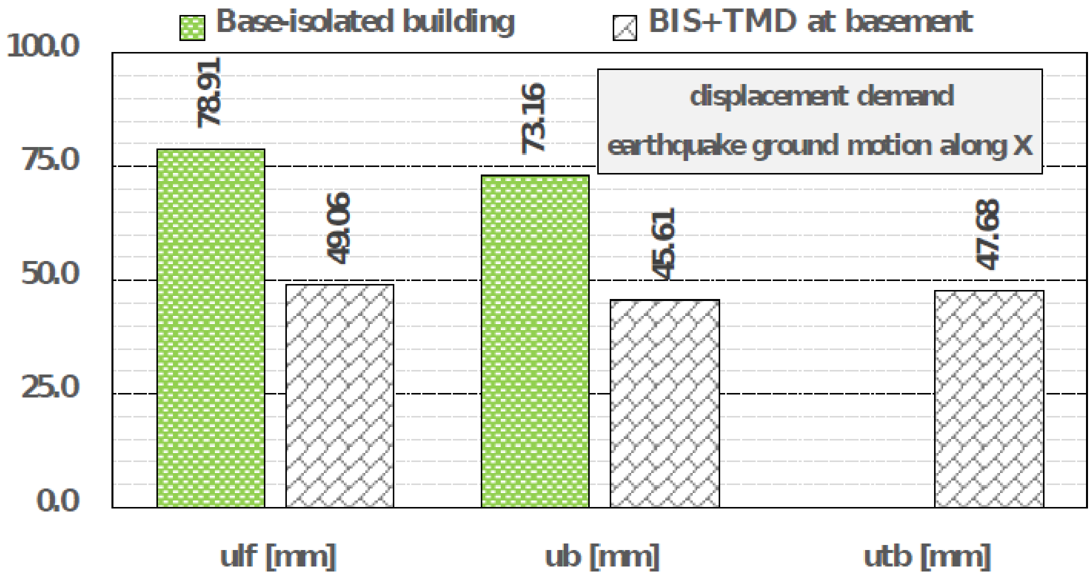

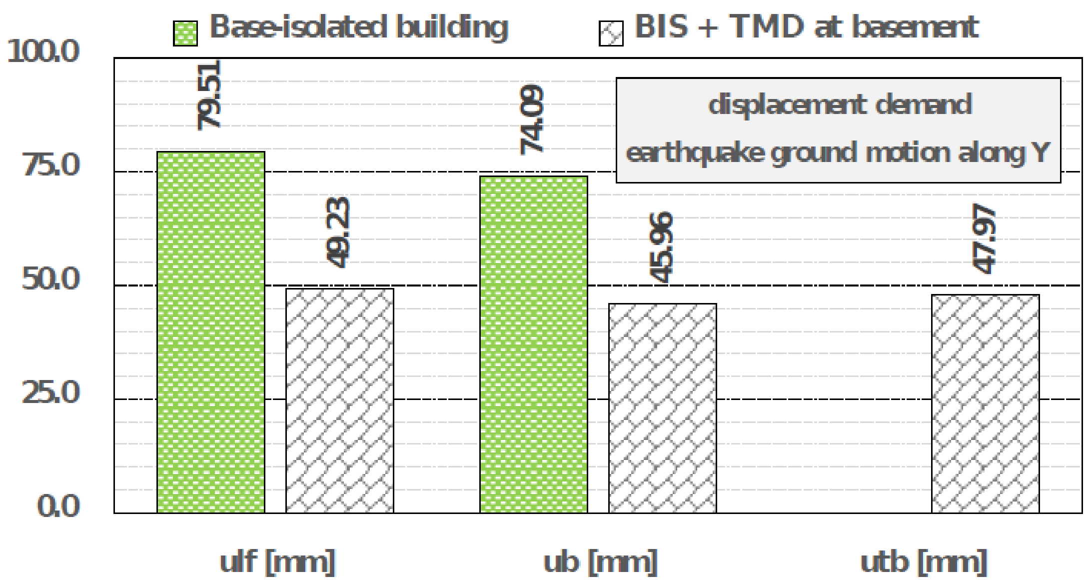

INERTER

Introduced to complete the force-current analogy between electrical and mechanical networks

Mechanical		Electrical	
$Y(s) = \frac{k}{s}$; $\frac{dF}{dt} = k(v_2 - v_1)$	Spring	$Y(s) = \frac{1}{Ls}$; $\frac{di}{dt} = \frac{1}{L}(v_2 - v_1)$	Inductor
$Y(s) = bs$; $F = b\frac{d(v_2 - v_1)}{dt}$	Inerter	$Y(s) = Cs$; $i = C\frac{d(v_2 - v_1)}{dt}$	Capacitor
$Y(s) = c$; $F = c(v_2 - v_1)$	Damper	$Y(s) = \frac{1}{R}$; $i = \frac{1}{R}(v_2 - v_1)$	Resistor

Smith (2002), Chen et al. (2009)

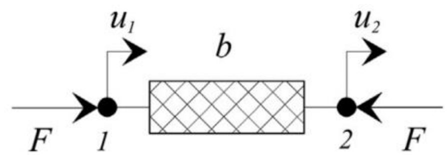

$$F = b(\ddot{u}_1 - \ddot{u}_2)$$

Inertance
(dimensions of mass [kg])

current ↔ force
voltage ↔ velocity
electrical ground ↔ mechanical ground

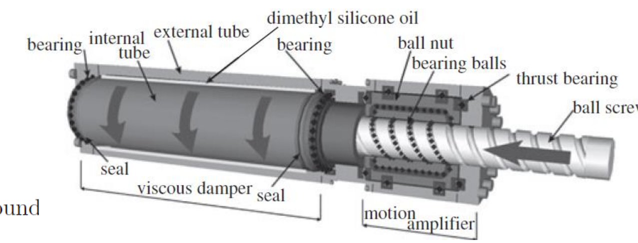

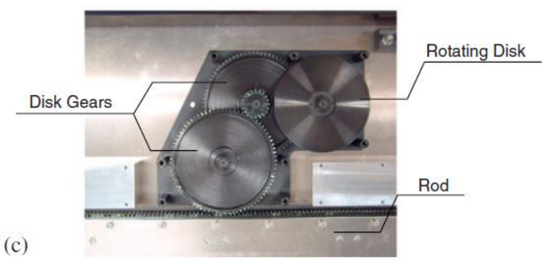

(c)

Mass amplification effect increased by adjusting the gearing ratios (traslational to rotational inertia conversion)

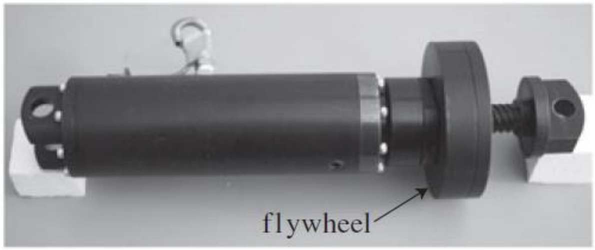

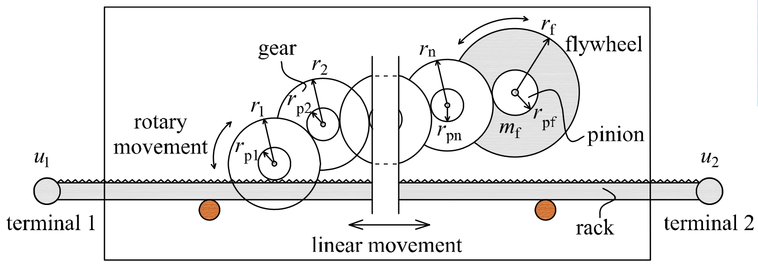

$$b = m_f \frac{r_f^2}{r_{pf}^2}\left(\prod_{i=1}^{n}\frac{r_i^2}{r_{pi}^2}\right)$$

Inerter presented in Ikago et al. (2012), Earth. Eng. Struct. Dyn. 41: 453-474

Mass: 2 kg
Inertance (apparent mass): 350 kg

Mass amplification = 175

INERTER

The inerter, under the name of J-damper, has been employed in the automotive sector for Formula 1 racing car suspensions (McLaren)

Kimi Raikkonen at the Spanish Grand Prix 2005 driving the McLaren MP4-20 to victory on the first racing deployment of the inerter

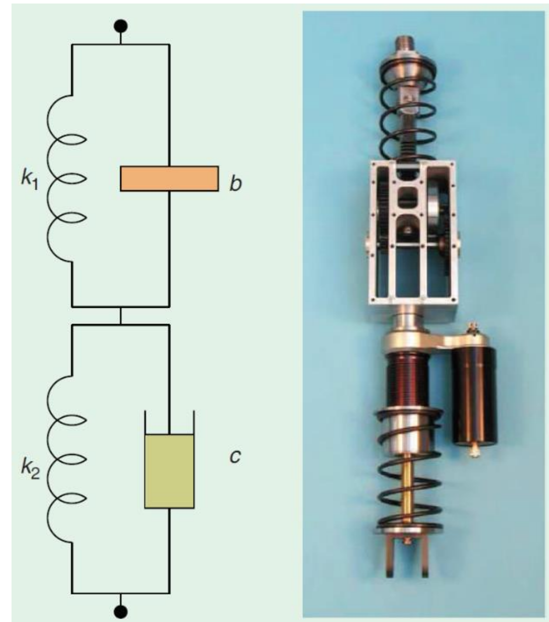

J-damper: inerter unit installed in series with damper with centring springs. The inerter is tuned to the tire natural frequency to maintain maximum tire contact patch area

TUNED MASS DAMPER INERTER (TMDI)

Exploiting the inerter to improve the performance of vibration absorbers / TMDs without implying enormous masses!

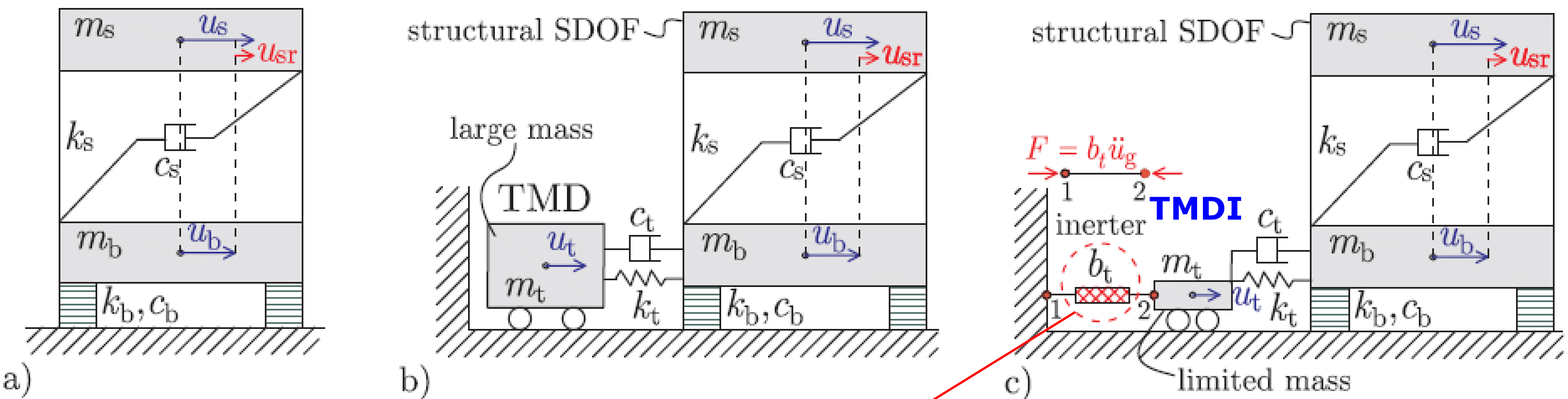

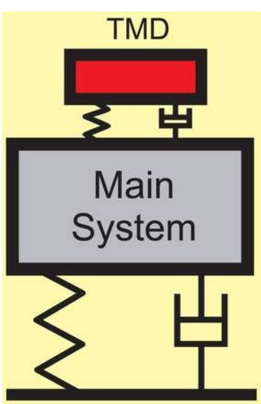

Traditional TMD

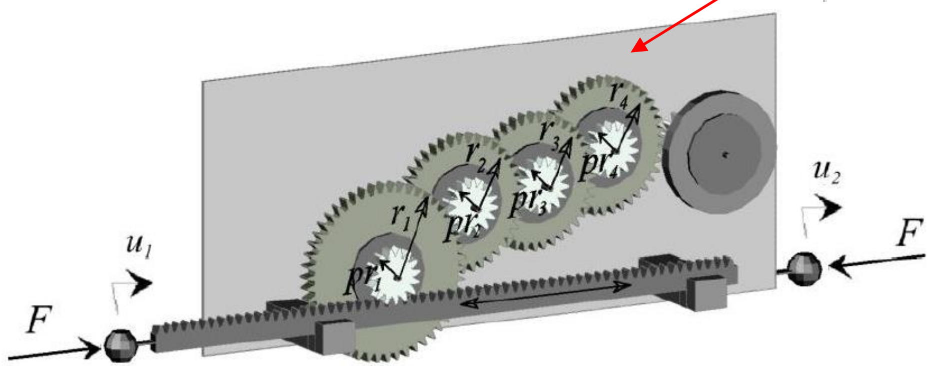

Inerter

INERTER + TMD

TMDI
Tuned Mass Damper Inerter

BIS + TMDI

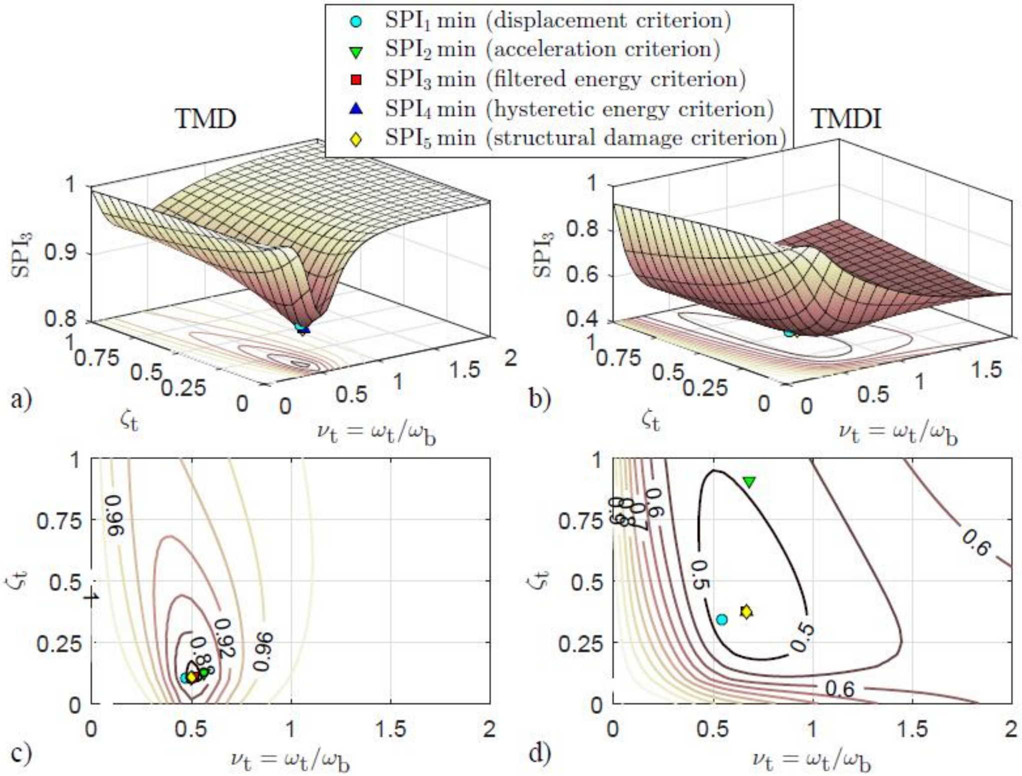

The TMDI system is more robust than the TMD to variations of the system parameters (e.g. reductions of hysteresis loops, degradation of effective stiffness, reduction of friction coefficient due to cycling effects, etc.)

Moreover, the TMD stroke is significantly reduced

De Domenico & Ricciardi
Earth Eng Struct Dyn, vol. 47(5) 2018
Earth Eng Struct Dyn, vol. 47(12) 2018

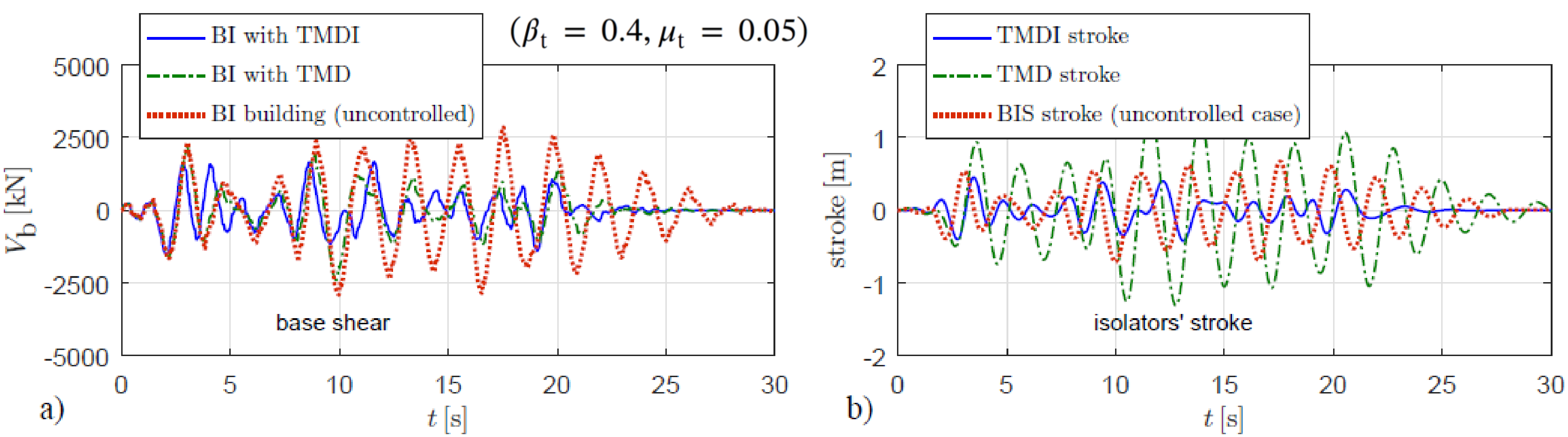

FLUID INERTER

Similar technology to fluid-viscous dampers (piston-cylinder mechanisms)

The linear motion of the piston conveys the fluid in an external helical channel, which produces rotational inertia of a fluid mass

Swift et al. (2013) Int J Contr. 86(11)
Glover et al. – Int. Patent 2009
Gartner & Smith – Int. Patent 2010

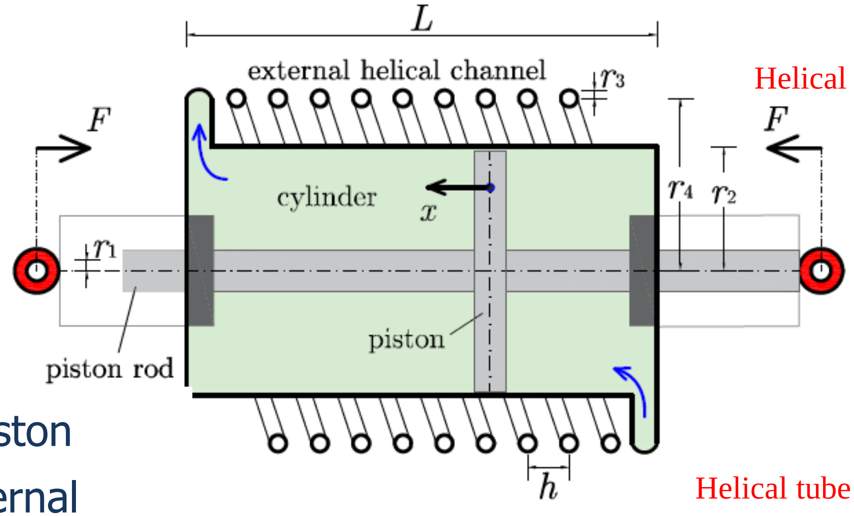

Helical tube co-axial to the cylinder

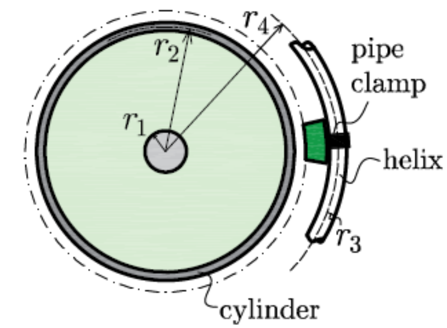

Helical tube external to cylinder

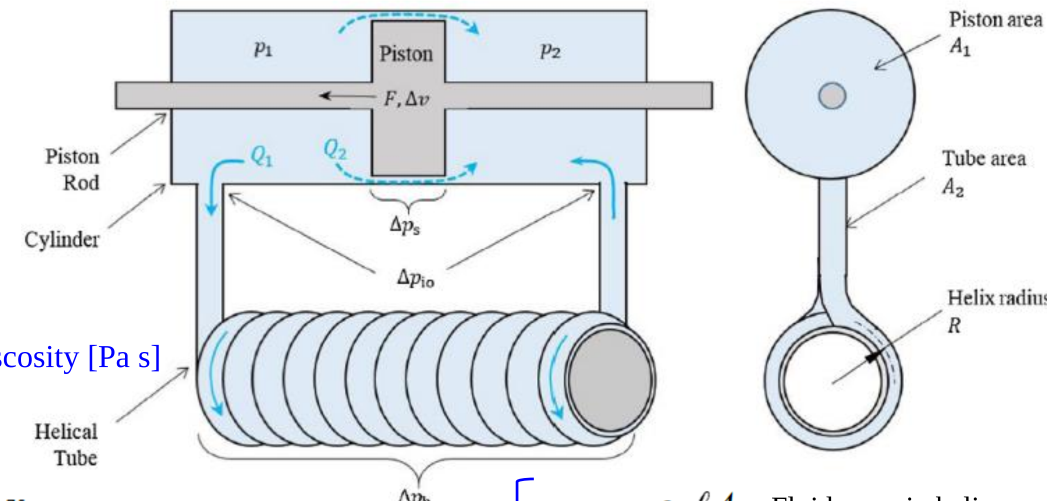

Dynamic viscosity [Pa s]

$$F_{\text{inerter}} = b\ddot{x} \quad \text{with} \quad b = \frac{m_{hel}}{1+(h/2\pi r_4)^2}\left(\frac{A_1}{A_2}\right)^2$$

$$F_{d-\text{helical}} = c_p^{NL}\dot{x}^{1.75} \quad \text{with} \quad c_p^{NL} = \frac{0.0664\mu_f^{0.25}\rho_f^{0.75}\ell A_1}{r_3^{1.25}}\left(\frac{A_1}{A_2}\right)^{1.75}$$

Mass density [kg/m³]

$$F_{d-\text{inlet}} = c_1\dot{x}^2 \quad \text{with} \quad c_1 = 0.25A_1\rho_f\left(\frac{A_1}{A_2}\right)^2; \quad F_{d-\text{outlet}} = c_2\dot{x}^2 \quad \text{with} \quad c_2 = 0.5A_1\rho_f\left(\frac{A_1}{A_2}\right)^2$$

$$F_{\text{shear}} = \frac{\mu_f 2\pi r_2 L}{\Delta r}\dot{x}$$

Darcy's formula for smooth pipe and turbulent flow

$m_{hel} \approx \rho_f \ell A_2$ Fluid mass in helix

$A_2 = \pi r_3^2$ Helical area

$A_1 = \pi(r_2^2 - r_1^2)$ Piston area

$$F = F_{\text{inerter}} + F_{\text{damping,tot}}$$

FLUID INERTER

Advantages over mechanical inerter:

1) *Piston-cylinder technology is widely used in earthquake engineering;*
2) *Reduction of backlash, ratcheting and other friction phenomena typical of mechanical gears;*
3) *Besides inertance, it provides a (parasitic) damping due to the pressure drops in helical channels (can be properly designed!)*

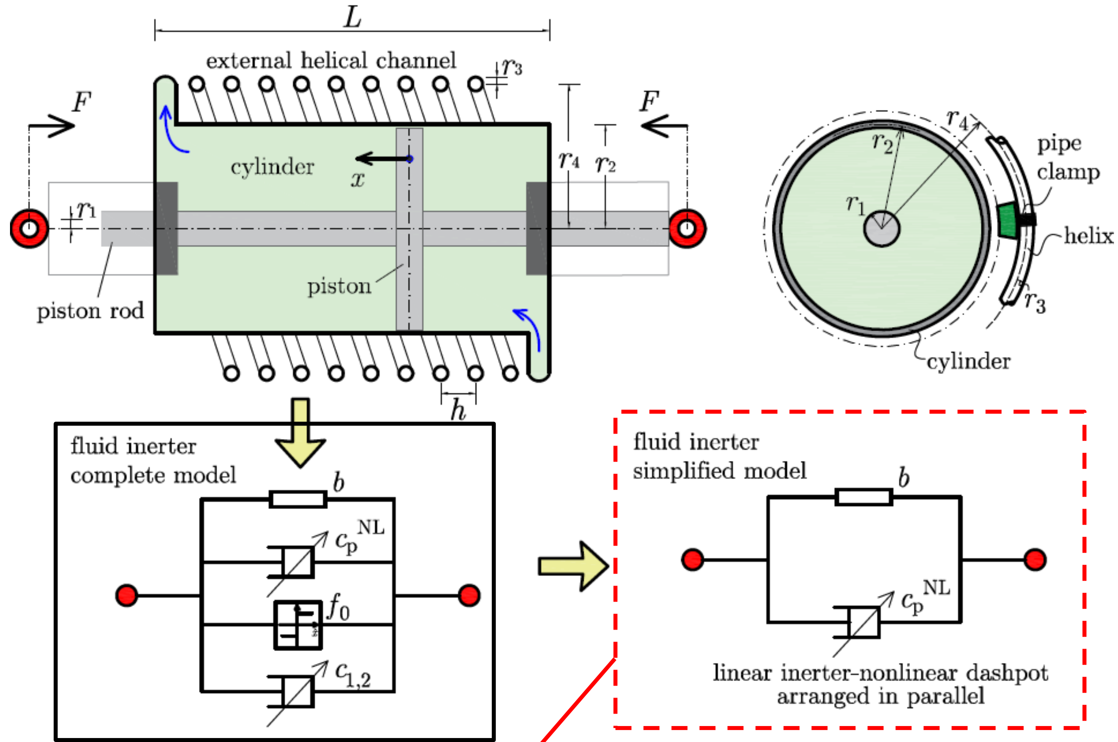

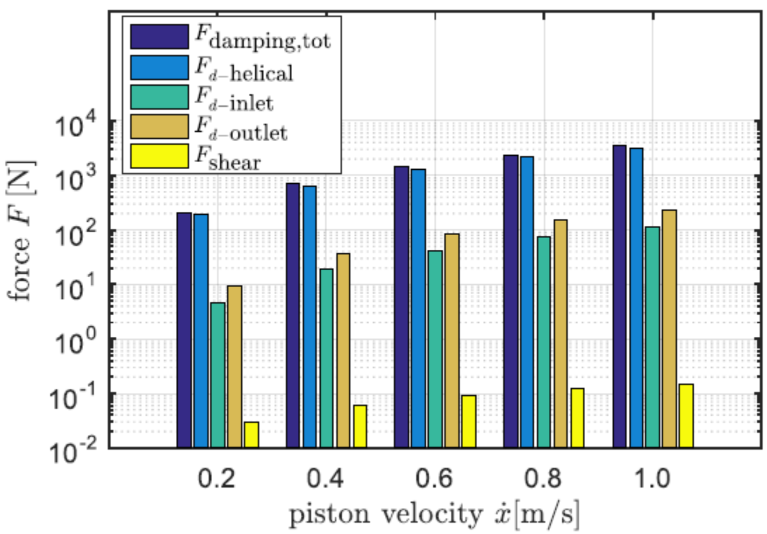

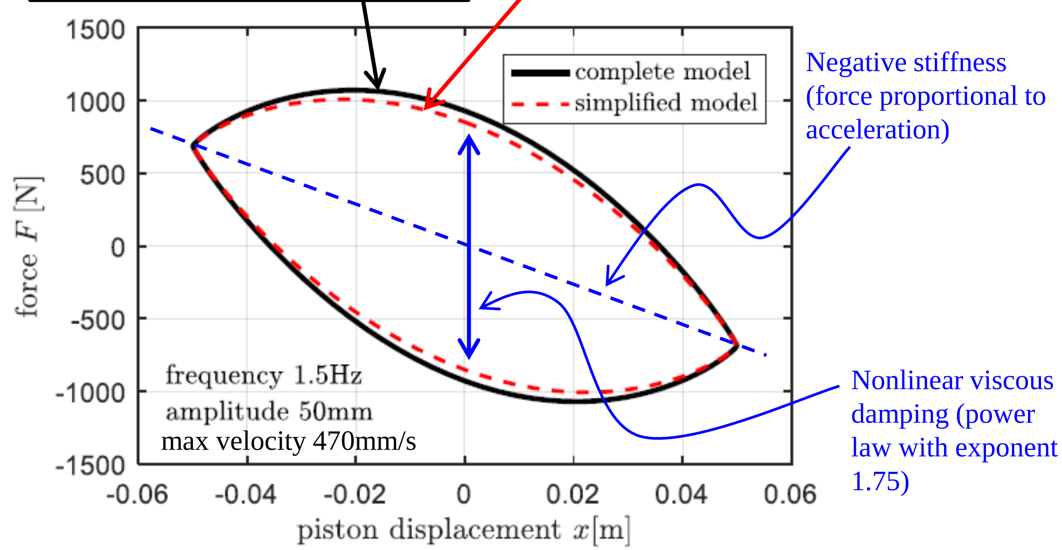

Fluid inerter data reported in Glover et al. – Int. Patent 2009 subjected to imposed sinsoidal motion

FLUID INERTER

Geometrical and physical parameters of the tested fluid inerter device.

Symbol [units]	Value	
r_1[m]	0.014	
r_2[m]	0.025	
r_2[m]	0.006	
r_4[m]	0.120	
h[m]	0.030	← pitch of helix
n_t[dimensionless]	7	← coils
ρ_f[kg/m^3]	802	} silicone oil
μ_f[Pa s]	0.00168	

Experimental tests at Dept. of Mechanical Engineering, University of Sheffield, UK

De Domenico, Deastra, Ricciardi, Sims, Wagg (2019) Journal of the Franklin Institute 356; 7626-7549

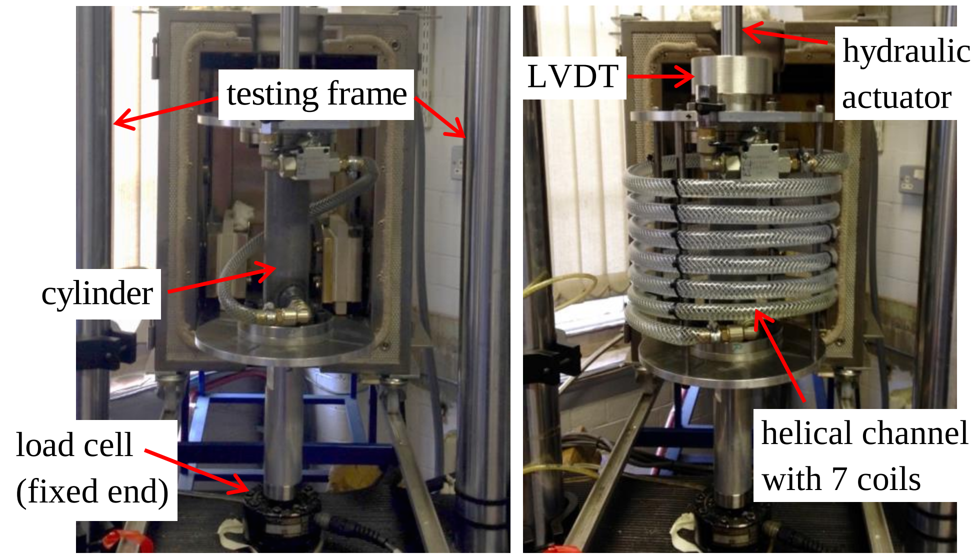

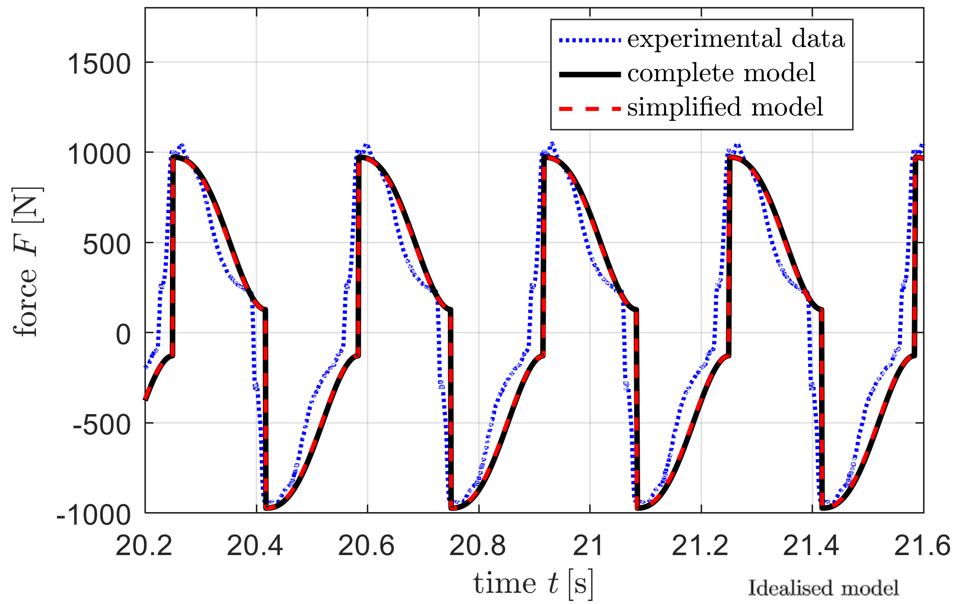

amplitude 17.5mm, frequency 3 Hz

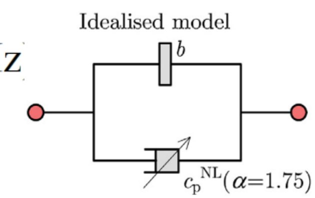

Simplified model is accurate enough to capture the experimental data…

→ The most important contribution to damping is due to the pressure drops in the helical channel, other terms can be neglected (shear friction, inlet, outlet, ecc.)

BIS + TUNED FLUID INERTER (TFI)

De Domenico, Ricciardi & Zhang (2020) Soil Dyn Earth Eng 132; 106099

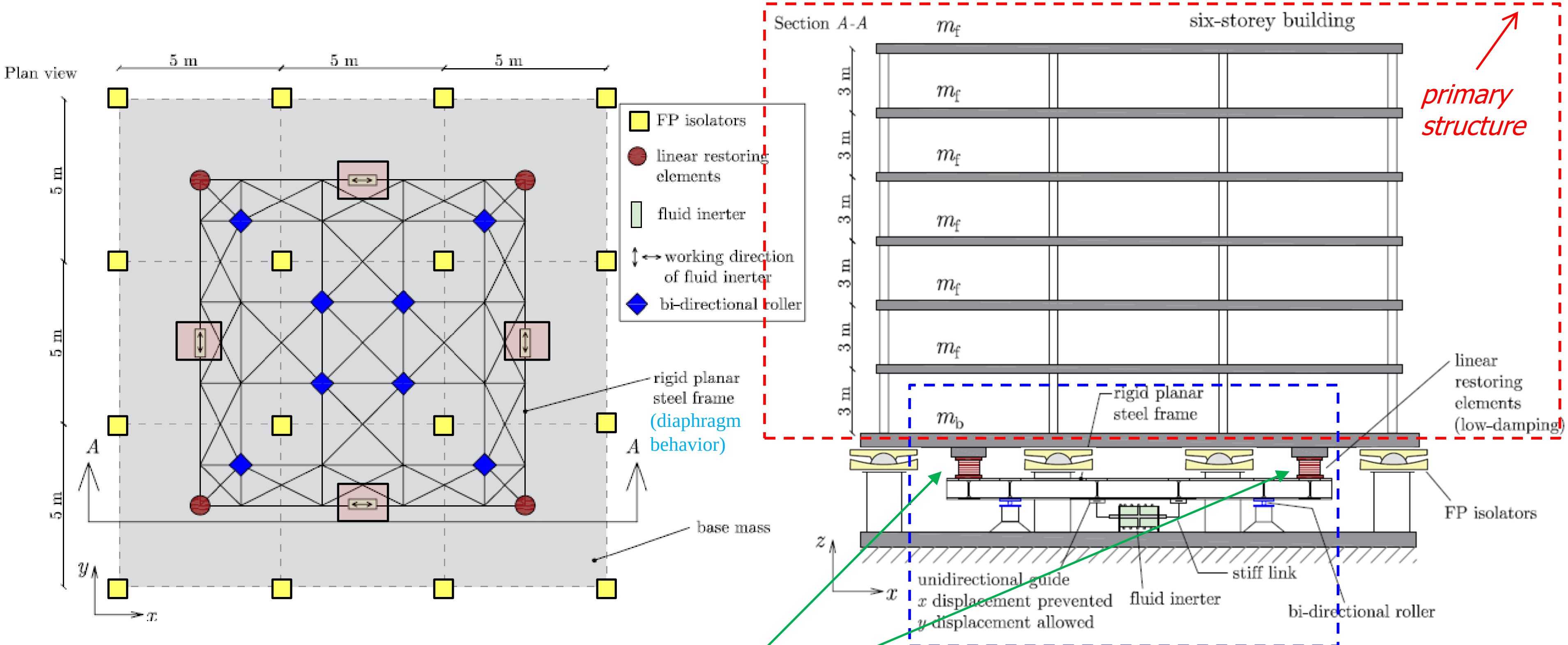

Exploit the inertial and damping properties of the fluid inerter in combination with base-isolation system (e.g. FPS bearings)

$$F_{FPS} = k_b u_b + f_b W_{tot}\,\mathrm{sgn}(\dot{u}_b)$$

Introduction of an auxiliary set of low-damping rubber bearings to connect the structure with the fluid inerter → tuned fluid inerter

$$F_{FI} = b\ddot{u}_t + c_p^{NL}\left|\dot{u}_t\right|^{1.75}\mathrm{sgn}(\dot{u}_t)$$

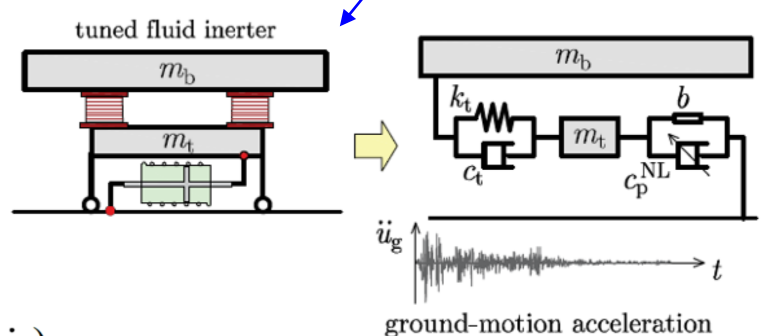

BIS + TUNED FLUID INERTER (TFI)

De Domenico, Ricciardi & Zhang (2020)
Soil Dyn Earth Eng 132; 106099

OPTIMAL DESIGN OF THE FLUID INERTER PARAMETERS

$$S_{\ddot{u}_g}(\omega) = \frac{\omega_g^4 + 4\zeta_g^2\omega_g^2\omega^2}{\left(\omega_g^2-\omega^2\right)^2 + 4\zeta_g^2\omega_g^2\omega^2}\,\frac{\omega^4}{\left(\omega_f^2-\omega^2\right)^2 + 4\zeta_f^2\omega_f^2\omega^2} S_w \qquad \text{with } S_w = \frac{0.141\zeta_g \ddot{u}_{g0}^2}{\omega_g\sqrt{1+4\zeta_g^2}}$$

Kanai-Tajimi + Clough-Penzien

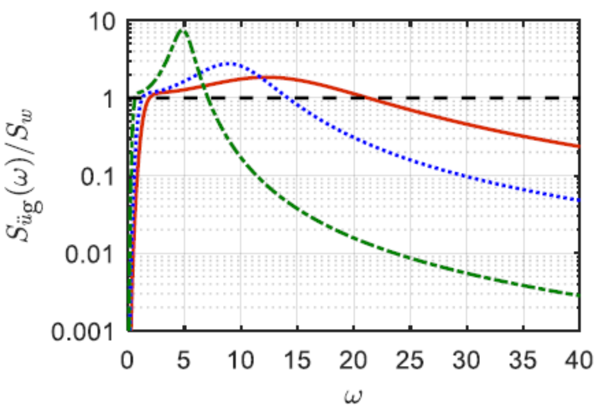

Der Kiureghian & Neuenhofer (1992)

Soil type	ω_g (rad/s)	ζ_g	ω_f (rad/s)	ζ_f
firm	15.0	0.6	1.5	0.6
medium	10.0	0.4	1.0	0.6
soft	5.0	0.2	0.5	0.6

- firm soil (broad-band excitation)
- medium soil
- soft soil (narrow-band excitation)
- white noise (extremely broad-band excitation)

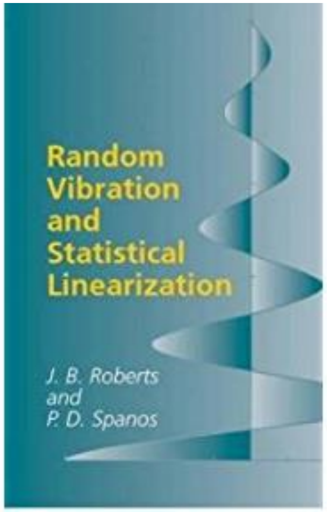

$$F_{FPS}^{SL} = k_b u_b + c_{b,eq}\dot{u}_b \qquad \text{FPS}$$

$$F_{FI}^{SL} = b\ddot{u}_t + c_{p,eq}\dot{u}_t \qquad \text{fluid inerter}$$

Stochastic linearization technique

$$\Sigma_{\dot{u}\dot{u}} = \mathrm{E}[\dot{\mathbf{u}}\dot{\mathbf{u}}^T] = \int_{-\infty}^{\infty} \omega^2 \mathbf{H}_U(\omega) S_{\ddot{u}_g}(\omega) \mathbf{H}_U(\omega)^{*T} \mathrm{d}\omega$$

$$c_{b,eq} = f_b W_{tot} E\left[\frac{\partial \operatorname{sgn}(\dot{u}_b)}{\partial \dot{u}_b}\right] = f_b W_{tot} E\left[2\delta(\dot{u}_b)\right] = f_b W_{tot}\sqrt{\frac{2}{\pi}}\frac{1}{\sigma_{\dot{u}_b}} \qquad \text{FPS}$$

$$c_{p,eq} = c_p^{NL}\frac{E[|\dot{u}_t|^{2.75}]}{E[\dot{u}_t^2]} = c_p^{NL}\frac{2^{1.375}\Gamma(1.875)}{\sqrt{\pi}}\sigma_{\dot{u}_t}^{0.75} = 1.3952\, c_p^{NL}\sigma_{\dot{u}_t}^{0.75} \qquad \text{fluid inerter}$$

input-output relationships in the frequency domain

Iterative procedure

BIS + TUNED FLUID INERTER (TFI)

De Domenico, Ricciardi & Zhang (2020)
Soil Dyn Earth Eng 132; 106099

OPTIMAL DESIGN OF THE FLUID INERTER PARAMETERS

$$\min_{\boldsymbol{\theta}} \mathrm{OF}(\boldsymbol{\theta}) \quad \mathrm{s.t.}\ \boldsymbol{\theta}_{\mathrm{lb}} \le \boldsymbol{\theta} \le \boldsymbol{\theta}_{\mathrm{ub}} \qquad \boldsymbol{\theta} = [\beta, \zeta_p^{NL}]$$

$$\beta = b / M_{\mathrm{tot}}$$

$$\zeta_p^{NL} = c_p^{NL} / 2\sqrt{k_{\mathrm{b}} M_{\mathrm{tot}}}$$

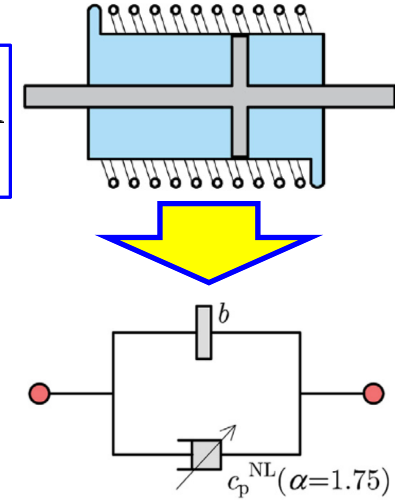

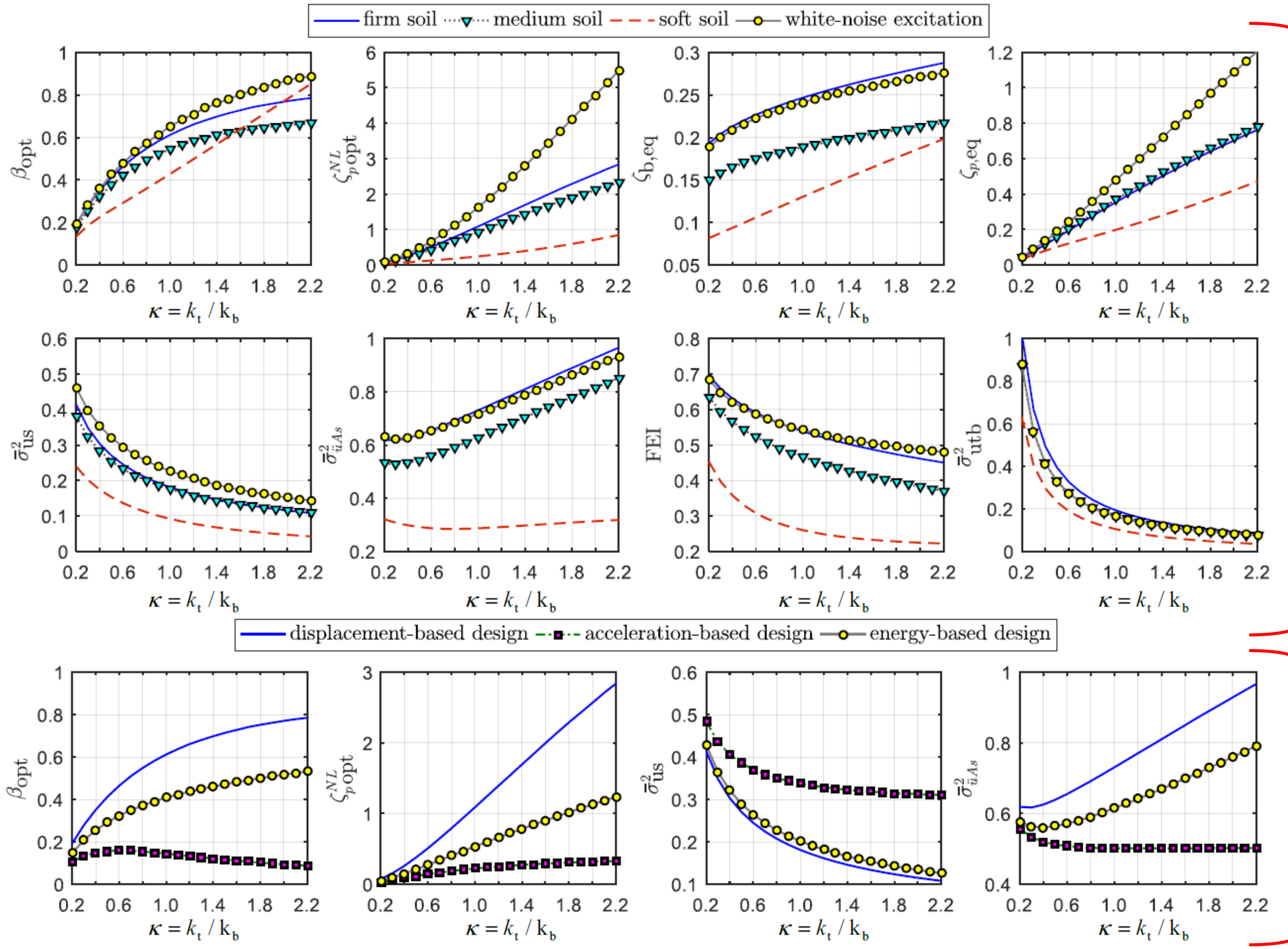

Depending on the soil conditions

Depending on the objective function

BIS + TUNED FLUID INERTER (TFI)

De Domenico, Ricciardi & Zhang (2020)
Soil Dyn Earth Eng 132; 106099

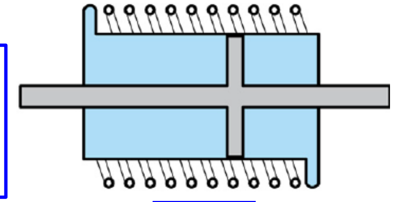

OPTIMAL DESIGN OF THE FLUID INERTER PARAMETERS

$$\min_{\boldsymbol{\theta}} \mathrm{OF}(\boldsymbol{\theta}) \quad \text{s.t. } \boldsymbol{\theta}_{\mathrm{lb}} \le \boldsymbol{\theta} \le \boldsymbol{\theta}_{\mathrm{ub}} \qquad \boldsymbol{\theta} = [\beta, \zeta_p^{NL}]$$

$$\beta = b / M_{\mathrm{tot}}$$

$$\zeta_p^{NL} = c_p^{NL} / 2\sqrt{k_{\mathrm{b}} M_{\mathrm{tot}}}$$

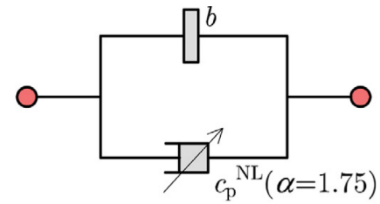

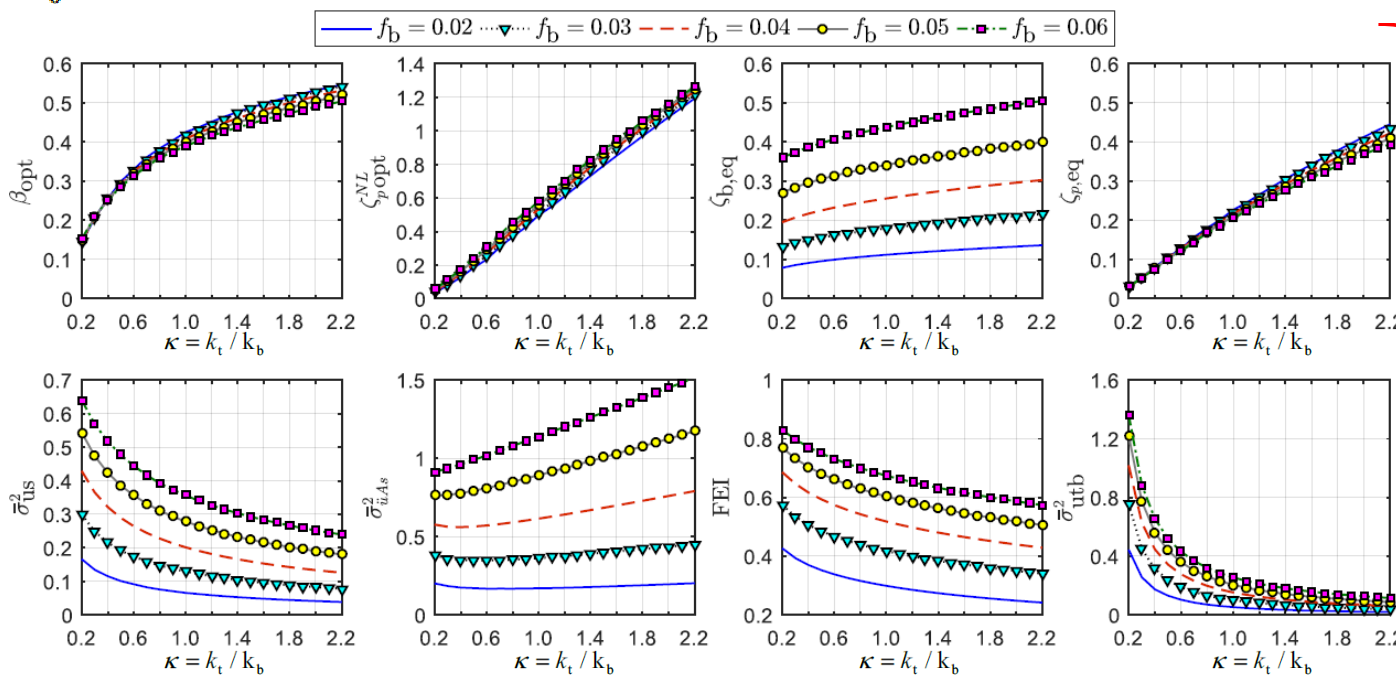

Depending on the friction coefficient of the FPS

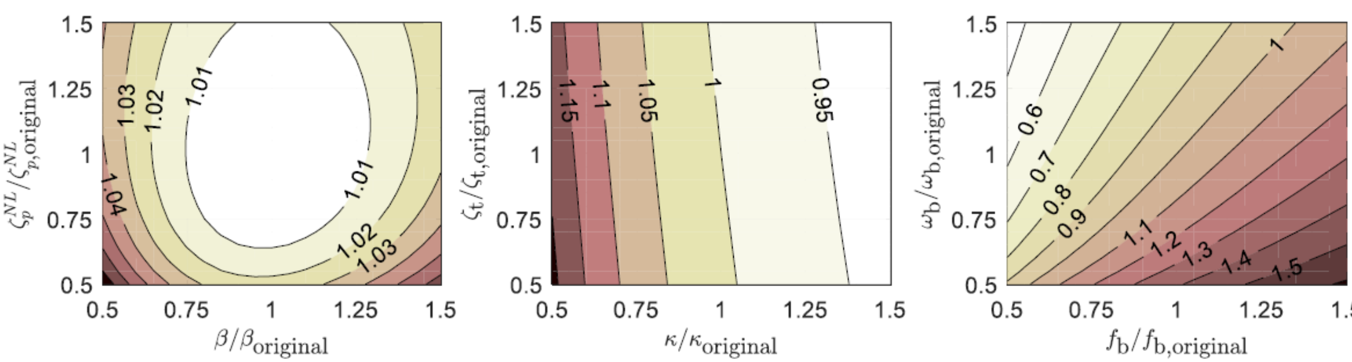

Sensitivity analysis to variation of system parameters

BIS + TUNED FLUID INERTER (TFI)

De Domenico, Ricciardi & Zhang (2020)
Soil Dyn Earth Eng 132; 106099

SEISMIC PERFORMANCE

100 accelerograms from FEMA P695 record set
44 far-field
56 near-fault of which 28 pulse-like and 28 non-pulse

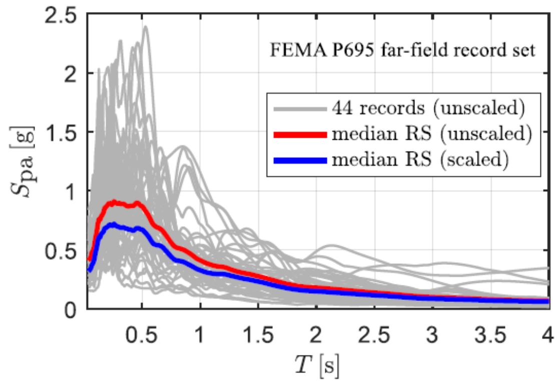

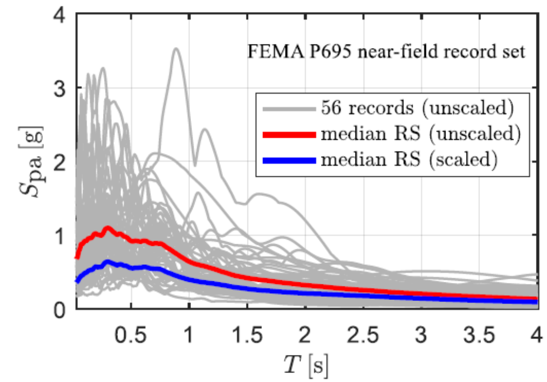

synthetically represents the pulse duration of the ground motion

6-story structure $T_{s1} \approx 0.50\,\mathrm{s}$

$m_1 = \ldots = m_6 = 100000\mathrm{kg}$

$k_1 = \ldots = k_6 = 270\mathrm{MN/m}$

base-isolated with FPS

$\omega_b = \pi \qquad f_b = 0.04$

auxiliary low-damping rubber bearings

$\kappa = 0.8 \qquad \zeta_t = 0.1$

optimal parameters of the fluid inerter from the optimization procedure

$\beta_{opt} = 0.372 \qquad \zeta_{p,opt}^{NL} = 0.403$

Record	PEER NGA RSN	Event name†	Type	PGA/PGV (1/s)	Record	PEER NGA RSN	Event name†	Type	PGA/PGV (1/s)
1	68	San Fernando	FF	10.8	26	723	Superstition Hills-02	NFP	3.9
2	125	Friuli, Italy-01	FF	11.1	27	802	Loma Prieta	NFP	6.7
3	169	Imperial Valley-06	FF	10.4	28	821	Erzican, Turkey	NFP	5.0
4	174	Imperial Valley-06	FF	8.8	29	828	Cape Mendocino	NFP	7.5
5	721	Superstition Hills-02	FF	7.6	30	879	Landers	NFP	5.5
6	725	Superstition Hills-02	FF	12.3	31	1063	Northridge-01	NFP	5.1
7	752	Loma Prieta	FF	14.9	32	1086	Northridge-01	NFP	5.8
8	767	Loma Prieta	FF	12.3	33	1165	Kocaeli, Turkey	NFP	7.2
9	827	Cape Mendocino	FF	12.3	34	1503	Chi-Chi, Taiwan	NFP	6.3
10	848	Landers	FF	9.7	35	1529	Chi-Chi, Taiwan	NFP	2.7
11	900	Landers	FF	4.6	36	1605	Duzce, Turkey	NFP	6.4
12	953	Northridge-01	FF	8.1	37	126	Gazli, USSR	NFNP	9.8
13	960	Northridge-01	FF	10.4	38	160	Imperial Valley-06	NFNP	16.8
14	1111	Kobe, Japan	FF	13.4	39	165	Imperial Valley-06	NFNP	9.0
15	1116	Kobe, Japan	FF	6.2	40	495	Nahanni, Canada	NFNP	26.4
16	1148	Kocaeli, Turkey	FF	5.5	41	496	Nahanni, Canada	NFNP	12.7
17	1158	Kocaeli, Turkey	FF	6.0	42	741	Loma Prieta	NFNP	11.2
18	1244	Chi-Chi, Taiwan	FF	3.8	43	753	Loma Prieta	NFNP	11.0
19	1485	Chi-Chi, Taiwan	FF	12.8	44	825	Cape Mendocino	NFNP	11.7
20	1602	Duzce, Turkey	FF	12.9	45	1004	Northridge-01	NFNP	10.2
21	1633	Manjil, Iran	FF	9.2	46	1048	Northridge-01	NFNP	7.7
22	1787	Hector Mine	FF	8.0	47	1176	Kocaeli, Turkey	NFNP	4.2
23	181	Imperial Valley-06	NFP	3.9	48	1504	Chi-Chi, Taiwan	NFNP	6.0
24	182	Imperial Valley-06	NFP	4.1	49	1517	Chi-Chi, Taiwan	NFNP	9.9
25	292	Irpinia, Italy-01	NFP	6.7	50	2114	Denali, Alaska	NFNP	2.6

† Each event collects two distinct horizontal components; FF: far-field record; NFP: near-field record with pulse; NFNP: near-field record with no-pulse

BIS + TUNED FLUID INERTER (TFI)

De Domenico, Ricciardi & Zhang (2020)
Soil Dyn Earth Eng 132; 106099

SEISMIC PERFORMANCE

100 accelerograms from FEMA P695 record set
44 far-field
56 near-fault of which 28 pulse-like and 28 non-pulse

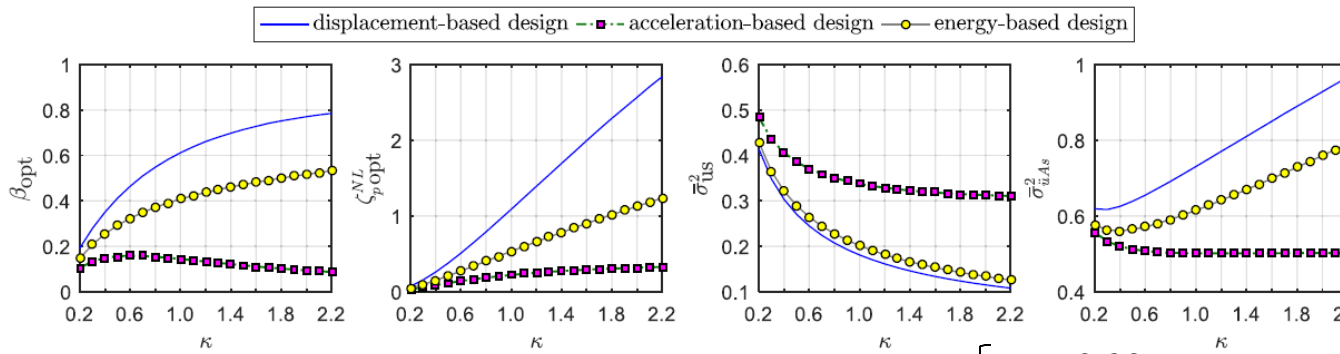

$\mu_t = 0.005$ *TMDI e TFI*

$\mu_t = 0.10$ *TMD*

Reduction of disp, IDRs and floor accelerations

Better performance than TMD with much higher mass (20 times higher!!)

For near-fault ground motions TFI better than TMDI

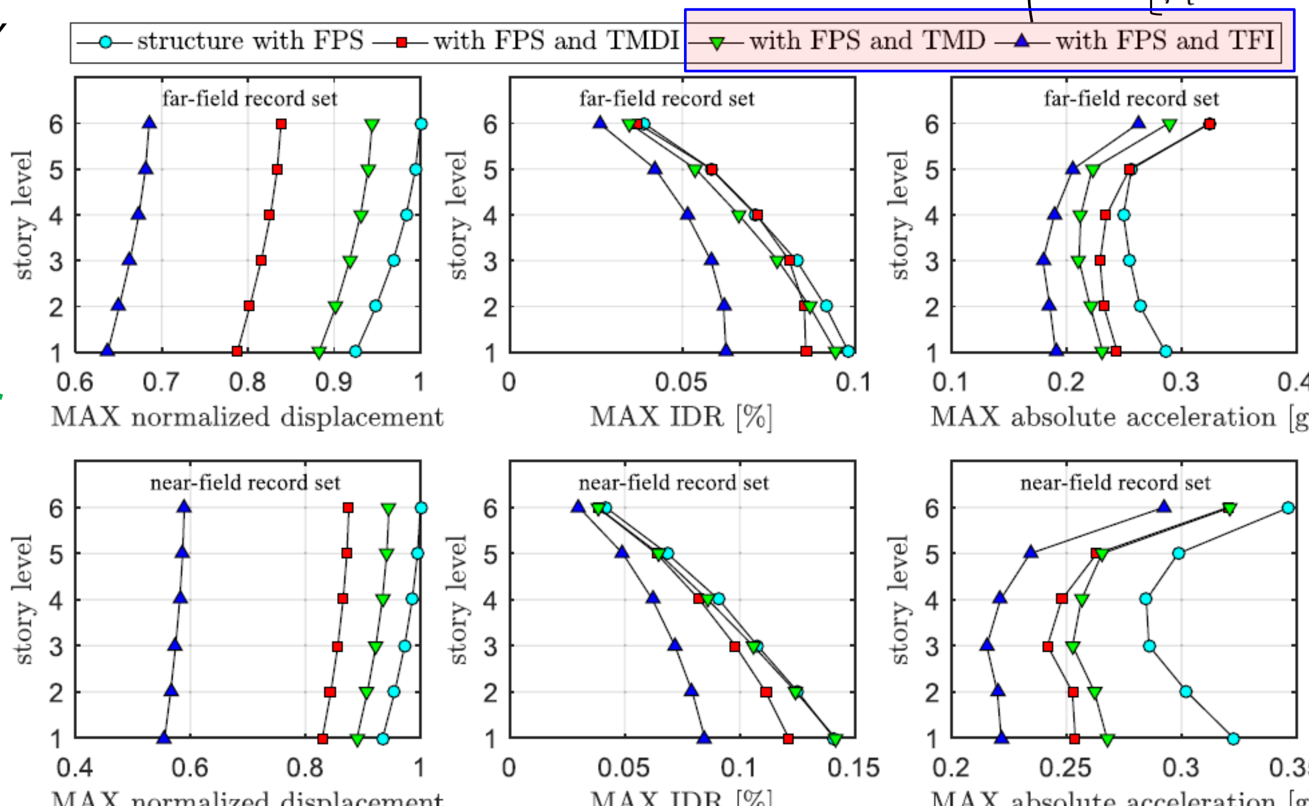

average MAX values for the two excitation classes (far-field vs near-field)

u_{red}>40%
acc_{red}>30%

DESIGN OF FLUID INERTER

De Domenico, Deastra, Ricciardi, Sims, Wagg (2019)
Journal of the Franklin Institute 356; 7626-7549

TARGET INERTANCE

$$b = 452{,}380 \text{ [kg]}$$

TARGET DAMPING

$$c_p^{NL} = 737{,}760 \text{ [N(s/m)}^{1.75}\text{]}$$

Target parameters from the optimization procedure

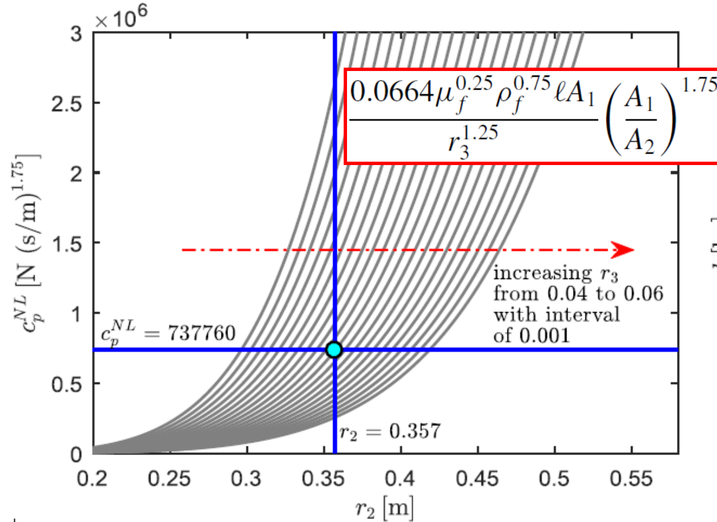

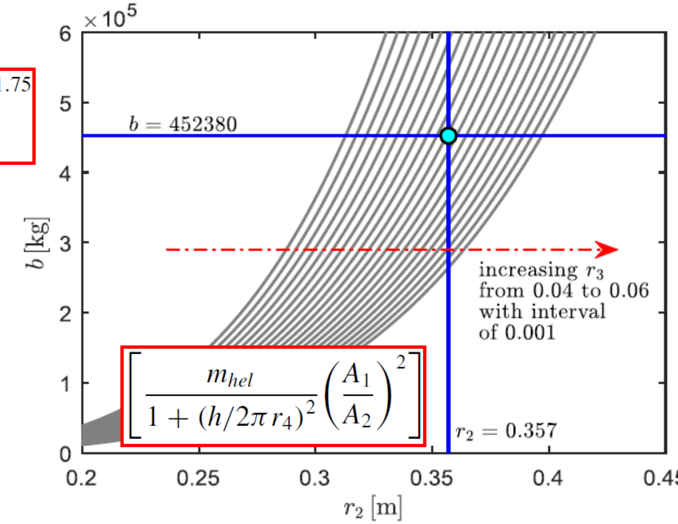

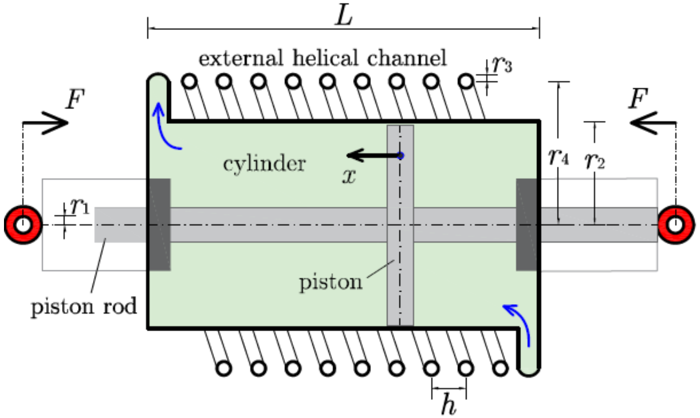

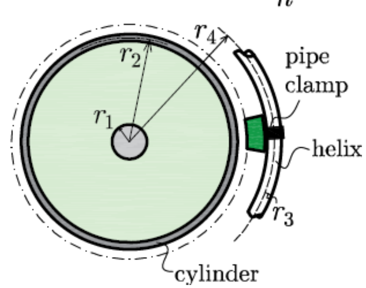

$$n_t = (L - 2r_3)/2r_3$$

$$h = 2r_3$$

$$r_d = r_4 - (r_2 + r_3)$$

gap between cylinder and helix (fixed to 6 cm)

$$r_2 = 0.357$$

$$r_3 = 0.05$$

inertance and damping are two coupled parameters that depend upon radius of helix and piston (A_1, A_2) in a complex manner…
use of design graphs facilitates the task

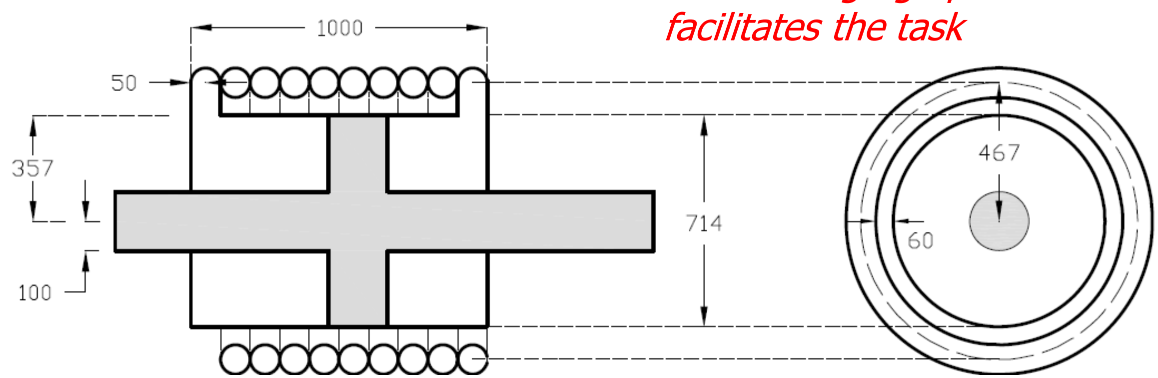

CONCLUSIONS

Mechanical inerter

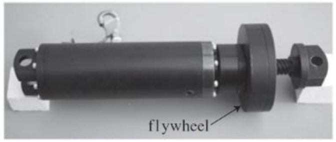

- ***Selectively modify the inertial properties of the structure without implying increase of seismic force (relative acc., not absolute!)***
- ***Can be used to improve performance of TMD systems (TMDI)***
- ***Can be used to improve performance and increase structural robustness of base-isolation systems***

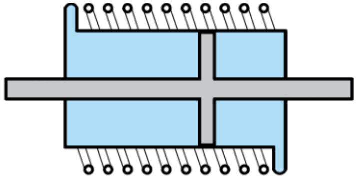

Fluid inerter

Same advantages as above, with the following additional considerations:

- ***Technology widely used in earthquake engineering (piston-cylinder)***
- ***Better performance compared to mechanical inerter for pulse-like ground motions due to the parasitic damping***
- ***Inertance and damping are coupled parameters, which complicates the design of the device (use of design graphs is convenient)***

ONGOING WORK

VALIDATION OF THE NUMERICAL WORK AGAINST EXPERIMENTAL EVIDENCE ON A REAL-SCALE PROTOTYPE IS DEFINITELY REQUIRED!

Laboratory CERISI, University of Messina, Italy

*Full-scale **3D** tests of isolators, and dissipation devices*

	Vertical	Longitudinal	Transversal
Force	16000 kN	±3100 kN	±1400 kN
Displacement	±35 mm	±550 mm	±375 mm
Speed	±55 mm/s	±1100 mm/s	±1100 mm/s
Rotation angle	±2°	±2°	±2°
Data acquisition rate	4 kS/s	4 kS/s	4 kS/s

UNIVERSITY OF MESSINA

UNIVERSITY "MEDITERRANEA" OF REGGIO CALABRIA

Thank you for your kind attention!

Dario De Domenico

dario.dedomenico@unime.it

Università degli Studi di Messina
DIPARTIMENTO DI INGEGNERIA